Okumura et al. Progress in Earth and Planetary Science (2016) 3:14
DOI 10.1186/s40645-016-0088-3

Progress in Earth and Planetary Science

RESEARCH ARTICLE Open Access

Hydrogen and carbon isotope systematics in hydrogenotrophic methanogenesis under H_2-limited and H_2-enriched conditions: implications for the origin of methane and its isotopic diagnosis

Tomoyo Okumura[1,2], Shinsuke Kawagucci[1,2,3*], Yayoi Saito[2,4], Yohei Matsui[2,3], Ken Takai[1,2,3] and Hiroyuki Imachi[2,3]

Abstract

Hydrogen and carbon isotope systematics of H_2O–H_2–CO_2–CH_4 in hydrogenotrophic methanogenesis and their relation to H_2 availability were investigated. Two H_2-syntrophic cocultures of fermentatively hydrogenogenic bacteria and hydrogenotrophic methanogens under conditions of $<10^2$ Pa-H_2 and two pure cultures of hydrogenotrophic methanogens under conditions of ~10^5 Pa-H_2 were tested. Carbon isotope fractionation between CH_4 and CO_2 during hydrogenotrophic methanogenesis was correlated with pH_2, as indicated in previous studies. The hydrogen isotope ratio of CH_4 produced during rapid growth of the thermophilic methanogen *Methanothermococcus okinawensis* under high pH_2 conditions (~10^5 Pa) was affected by the isotopic composition of H_2, as concluded in a previous study of *Methanothermobacter thermautotrophicus*. This "δD_{H_2} effect" is a possible cause of the diversity of previously reported values for hydrogen isotope fractionation between CH_4 and H_2O examined in H_2-enriched culture experiments. Hydrogen isotope fractionation between CH_4 and H_2O, defined by $(1000 + \delta D_{CH_4})/(1000 + \delta D_{H_2O})$, during hydrogenotrophic methanogenesis of the H_2-syntrophic cocultures was in the range 0.67–0.69. The hydrogen isotope fractionation of our H_2-syntrophic dataset overlaps with those obtained not only from low-pH_2 experiments reported so far but also from natural samples of "young" methane reservoirs (0.66–0.74). Conversely, such hydrogen isotope fractionation is not consistent with that of "aged" methane in geological samples (≥0.79), which has been regarded as methane produced via hydrogenotrophic methanogenesis from the carbon isotope fractionation. As a possible process inducing the inconsistency in hydrogen isotope signatures between experiments and geological samples, we hypothesize that the hydrogen isotope signature of CH_4 imprinted at the time of methanogenesis, as in the experiments and natural young methane, may be altered by diagenetic hydrogen isotope exchange between extracellular CH_4 and H_2O through reversible reactions of the microbial methanogenic pathway in methanogenic region and/or geological methane reservoirs.

Keywords: Methane, Hydrogenotrophic methanogenesis, Hydrogen isotope ratio, Carbon isotope ratio, H_2 availability, Culture experiments

* Correspondence: kawagucci@jamstec.go.jp
[1]Laboratory of Ocean-Earth Life Evolution Research (OELE), Japan Agency for Marine-Earth Science and Technology (JAMSTEC), 2-15 Natsushima-cho, Yokosuka 237-0061, Japan
[2]Department of Subsurface Geobiological Analysis and Research (D-SUGAR), Japan Agency for Marine-Earth Science and Technology (JAMSTEC), 2-15 Natsushima-cho, Yokosuka 237-0061, Japan
Full list of author information is available at the end of the article

Springer Open

© 2016 Okumura et al. **Open Access** This article is distributed under the terms of the Creative Commons Attribution 4.0 International License (http://creativecommons.org/licenses/by/4.0/), which permits unrestricted use, distribution, and reproduction in any medium, provided you give appropriate credit to the original author(s) and the source, provide a link to the Creative Commons license, and indicate if changes were made.

Background

Methane is a greenhouse gas, a primary product of methanogenic archaea, a useful fuel for human activity, and the simplest organic molecular. The geochemical origins of methane in environmental samples have been investigated in terms of global warming (e.g., Patra et al. 2011), limits of the deep biosphere (e.g., Inagaki et al. 2015), exploration and development of energy resources (e.g., Kvenvolden 1988), and prebiotic chemical evolution on the early Earth (e.g., McCollom 2013). The geochemical origin of methane can be classified into four types in terms of the carbon source (inorganic vs. organic) and the generation process (chemical vs. microbial): abiotic, thermogenic, aceticlastic and methylotrophic, and hydrogenotrophic methane (e.g., Kawagucci et al. 2013a). Because hydrogenotrophic methanogenesis is one of the most important energy metabolisms in living ecosystems in the ancient Earth and habitable extraterrestrial environments (McCollom 1999; Takai et al. 2004; Hsu et al. 2015), distinguishing hydrogenotrophic methanogenesis from the other methanogenic processes is a key to discuss whether life is present or absent there.

The stable isotope ratios of carbon ($^{13}C/^{12}C$) and hydrogen (D/H) in methane have been used as geochemical tracers to deduce its origin (e.g., Schoell 1980; 1988; Whiticar et al. 1986; Whiticar 1999). Although the usefulness of the stable isotope tracers for methane origins have been long debated (Martini et al. 1996; Waldron et al. 1999; Tang et al. 2000), the stable isotope diagnosis becomes more accurate by enhancing the understanding of stable isotope systematics with respect to each of the methanogenic processes in addition to subsequent alteration of the imprinted isotope signature. For this purpose, carbon isotope fractionation between CH_4 and CO_2 in hydrogenotrophic methanogenesis has been well studied by laboratory incubations (e.g., Valentine et al. 2004; Penning et al. 2005; Takai et al. 2008). The magnitude of the carbon isotope fractionation is thought to depend on the thermodynamic state of the methanogenic environment: a greater ^{13}C-depletion in the produced CH_4 occurs at a lower H_2 availability. This relationship has been explained by "differential reversibility" in the multistep pathway of methanogenesis from H_2 and CO_2 (Valentine et al. 2004): higher reversibility exhibits at a lower H_2 availability.

In contrast to the carbon isotopic characteristics, the hydrogen isotope characteristics of hydrogenotrophic methanogenesis remain less understood. In general, the hydrogen isotope ratio of produced CH_4 is related solely to that of H_2O (e.g., Daniels et al. 1980). Based on this finding, numerous studies have examined the CH_4–H_2O hydrogen isotope fractionation both in experiments using various methanogen cultures (Balabane et al. 1987; Sugimoto and Wada 1995; Valentine et al. 2004; Yoshioka et al. 2008; Hattori et al. 2012; Stolper et al. 2015; Wang et al. 2015) and by observations on methane-bearing environments (e.g., Nakai et al. 1974; Whiticar et al. 1986; Burke 1993; Waldron et al. 1999). Large variation of the CH_4–H_2O hydrogen isotope fractionation has been reported in previous studies (Additional file 1), and the possible relationship between the fractionation and the H_2 availability in the methanogenic environment has been discussed (Burke 1993; Yoshioka et al. 2008; Hattori et al. 2012; Stolper et al. 2015; Wang et al. 2015). On the other hand, Kawagucci et al. (2014) recently demonstrated that the hydrogen isotope ratio of substrate H_2 also affects the hydrogen isotope ratio of the produced CH_4 during the rapid growth of a thermophilic methanogen, *Methanothermobacter thermautotrophicus* strain ΔH, in H_2-enriched batch culture. If this "δD_{H2} effect" occurs ubiquitously in other hydrogenotrophic methanogens and under other growing conditions such as low H_2 availability, it may be necessary to reconsider the geochemical implications of the traditional interpretation based on the CH_4–H_2O hydrogen isotope ratio fractionation.

In this study, we therefore investigated the hydrogen and carbon isotope systematics of H_2O–H_2–CO_2–CH_4 during the growth of different hydrogenotrophic methanogens under various growth conditions and the effect of H_2 availability. We tested two different species of methanogens under syntrophic growth conditions with fermentatively hydrogenogenic bacteria that attained very low H_2 availability (corresponding to $<10^2$ Pa-H_2 in the headspace gas) and two different species of hydrogenotrophic methanogens under H_2-enriched growth conditions (~10^5 Pa-H_2 in the headspace gas). This is the first attempt to monitor both hydrogen and carbon isotope systematics in low-pH_2 cultures, although the hydrogen and carbon isotope systematics have been investigated separately (Penning et al. 2005; Yoshioka et al. 2008) (Additional file 1). Compilation of the hydrogen and carbon isotope fractionations from the experimental results and environmental observations reveals three provinces in the dataset and provides new insights into stable isotope diagnosis of the origin and fate of environmental methane.

Methods

Organism details and medium compositions

Table 1 provides information on the four culture sets and the experimental conditions used in this study. To assess the growth of methanogens under low H_2-availability conditions at different temperatures, two species of butyrate-oxidizing hydrogenogenic fermentative bacteria were cocultured with two species of methanogens as syntrophic consortia at 55 °C and 25 °C (thermophilic and mesophilic cocultures). The partial pressure of H_2 for the cocultures was lower than 10^2 Pa-H_2 during the

Table 1 Experimental and organismal information examined in this study

Culture type	T (°C)	Head space H_2 (Pa)	CH_4 substrate	Organism information	
				Syntrophic bacteria	Methanogen
Thermophilic coculture	55	$<6.0 \times 10^1$	Butyrate	*Syntrophothermus lipocalidus* (DSMZ 12681)	*Methanothermobacter thermautotrophicus* strain ΔH (JCM10044)
Mesophilic coculture[a]	25	$<1.0 \times 10^1$	Butyrate	*Syntrophomonas* sp.	*Methanobacterium* sp. strain MO-MB1
Thermophilic pure culture	60	$<2.1 \times 10^5$	H_2/CO_2	–	*Methanothermococcus okinawensis* strain IH1 (JCM11175)
Mesophilic pure culture	30	$<2.2 \times 10^5$	H_2/CO_2	–	*Methanobacterium* sp. strain MO-MB1

[a]The mesophilic coculture included a contaminant bacterium, *Geosporobacter* sp. (Saito et al. 2014)

incubation (see Results). In addition to the coculture sets, two hydrogenotrophic methanogen species were grown as pure culture under high H_2-availability conditions at 60 °C and 30 °C (thermophilic and mesophilic pure cultures). The initial partial pressure of H_2 for the pure culture sets was $2.0–2.2 \times 10^5$ Pa-H_2. The metabolic reactions in the culture sets are as follows:

$4H_2 + CO_2 \rightarrow CH_4 + 2H_2O$
(R1: Hydrogenotrophic methanogenesis),
$CH_3CH_2CH_2COO^- + 2H_2O \rightarrow 2CH_3COO^- + H^+ + 2H_2$
(R2: Butyrate oxidation),
$2CH_3CH_2CH_2COO^- + 2H_2O + CO_2 \rightarrow 4CH_3COO^- + 2H^+ + CH_4$
(R3: Consortium).

For the thermophilic coculture experimental set (hereafter, TC), we purchased a pure coculture of *Syntrophothermus lipocalidus* strain TGB-C1 and *Mtb. thermautotrophicus* strain ΔH (DSM 12681) from Deutsche Sammlung von Mikroorganismen und Zellkulturen (DSMZ; Braunschweig, Germany). *Mtb. thermautotrophicus* is one of the best-studied methanogens in terms of its genetic, biochemical, and biogeochemical characteristics (e.g., Smith et al. 1997; Kawagucci et al. 2014). *S. lipocalidus* was originally isolated from a granular sludge in a thermophilic upflow anaerobic sludge blanket reactor (Sekiguchi et al. 2000). The syntrophism between these microbes was previously studied by Sekiguchi et al. (2000). In addition, the CH_4–H_2O hydrogen isotope fractionation for this syntrophic consortium has been previously investigated (Yoshioka et al. 2008). The syntrophic consortium was cultivated in the medium as follows (L^{-1}): 0.54 g NH_4Cl, 0.14 g KH_2PO_4, 0.20 g $MgCl_2$–$6H_2O$, 0.15 g $CaCl_2$–$2H_2O$, 25 g NaCl, 2.0 g $NaHCO_3$, 0.5-mL resazurin solution (1 g L^{-1}), 1-mL vitamin solution, and 1-mL trace element solution. The composition of the vitamin solution was as follows (L^{-1}): 4.88 mg biotin, 8.82 mg folic acid, 4.12 mg pyridoxine–HCl, 6.74 mg thiamine–HCl, 7.52 mg riboflavin, 2.44 mg nicotinamide, 9.54 mg calcium pantothenate, 27.1 mg vitamin B12, 2.74 mg 4-aminobenzic acid, and 4.12 mg lipoic acid. The trace element solution contained (L^{-1}) the following composition: 1.27 g $FeCl_2$–$4H_2O$, 0.20 g $MnCl_2$–$4H_2O$, 0.13 g $CoCl_2$, 0.14 g $ZnCl_2$, 1.3 mg $CuCl_2$–$2H_2O$, 13.3 mg $AlCl_3$, 6.2 mg H_3BO_3, 24.2 mg Na_2MoO_4–$2H_2O$, 13.0 mg $NiCl_2$, 1.7 mg Na_2SeO_3, and 3.3 mg Na_2WO_4–$2H_2O$. Batches of the culture in 120-mL serum bottles, each containing 40 mL of medium, were flushed with mixture gas of N_2/CO_2 (80:20, v/v) for 5 min and sealed with butyl rubber septums and aluminum crimp seals. After autoclaving at 121 °C for 20 min, the headspace was pressurized with N_2 gas up to 150 kPa. After gas injection, 0.5 mL of the filter-sterilized reducing solution was added to the bottles. The reducing solution contained (L^{-1}) 6.25 g Na_2S–$9H_2O$ and 6.25 g cysteine-HCl. Butyrate solution sterilized in an autoclave was added to the culture bottles at a final concentration of 20 mmol/L immediately before the inoculation. The amount of inoculum for each TC batch was 0.55 mL. Batches of TC were incubated at 55 °C in the dark without shaking.

For the mesophilic coculture experimental set (hereafter, MC), we used a butyrate-oxidizing enrichment culture from our laboratory. The culture was obtained from subseafloor sediments collected off the Shimokita Peninsula, Japan (Imachi et al. 2011; Saito et al. 2014). The culture is a highly purified enrichment culture that constitutes only three types of microorganism: a mesophilic hydrogenotrophic methanogen, *Methanobacterium* sp. strain MO-MB1; a mesophilic butyrate-oxidizing hydrogenogenic bacterium, *Syntrophomonas* sp.; and a heterotrophic anaerobic bacterium, *Geosporobacter* sp. The procedure for culture batch preparation for MC was almost the same as that for TC with some differences, as follows. The base medium composition for MC was as follows (L^{-1}): 0.54 g NH_4Cl, 0.10 g KH_2PO_4, 4.0 g $MgCl_2$–$6H_2O$, 1.0 g $CaCl_2$–$2H_2O$, 25 g NaCl, 2.0 g $NaHCO_3$, 0.5-mL resazurin solution (1 g L^{-1}), 1-mL vitamin solution, and 1-mL trace element solution. The butyrate solution was added to the bottles at a final concentration of 10 mmol/L. The amount of inoculum for each MC batch was 1.5 mL. Batches of MC were incubated at 25 °C without shaking in the dark. The preliminary experiment showed that the growth of the consortium was optimal at 25 °C with minimum growth of the contaminant bacterium *Geosporobacter* sp. (Saito et al. 2014). We also confirmed that butyrate

oxidation occurred together with methane production stoichiometrically, which is explained by the eq. R1, 2, and 3 (see Additional file 2).

For the thermophilic pure culture experimental set (hereafter, TP), we used a thermophilic hydrogenotrophic methanogen, *Methanothermococcus okinawensis* strain IH1 (JCM 11175), from the culture collection of JAMSTEC. *Mtc. okinawensis* was isolated from a deep-sea hydrothermal vent chimney at the Iheya Ridge, Okinawa Trough (Takai et al. 2002). The base medium composition for TP was as follows (L^{-1}): 0.09 g KH_2PO_4, 0.09 g K_2HPO_4, 3.0 g $MgCl_2$–$6H_2O$, 4.0 g $MgSO_4$–$7H_2O$, 0.8 g $CaCl_2$, 0.33 g KCl, 30 g NaCl, 0.25 g NH_4Cl, 10.0 mg $NiCl_2$–$6H_2O$, 0.24 mg Na_2MoO_4–$2H_2O$, 4.9 mg $NaSeO_4$, 10.0 mg $Fe_2(SO_4)_3$, 0.5-mL resazurin solution (1 g L^{-1}), 10-mL trace element solution, and 2.5 g $NaHCO_3$. The trace element solution contained (L^{-1}): 1.0 g NaCl, 0.5 g $MnSO_4$–H_2O, 0.18 g $CoSO_4$–$2H_2O$, 0.1 g $CaCl_2$–$2H_2O$, 0.18 g $ZnSO_4$–$7H_2O$, 0.01 g $CuSO_4$–$5H_2O$, 0.02 g $KAl(SO_4)_2$–$12H_2O$, 0.01 g H_3BO_3, 0.025 g $NiCl_2$–$6H_2O$, and 0.3 mg Na_2SeO_3–$5H_2O$. Batches of the culture in 160-mL pressure-resistant serum bottles, each containing 20 mL of medium, were flushed with N_2 for 5 min, sealed with butyl rubber septums and aluminum crimp seals, and autoclaved at 121 °C for 20 min. The headspace for the TP comprised 100 kPa N_2, 100 kPa CO_2, and 200 kPa H_2. The medium was reduced by the addition of autoclaved 5 % (w/v) Na_2S–$9H_2O$ solution to a final concentration of 2.1 mmol/L. The amount of inoculum for each TP batch was 0.1 mL. Batches of TP were incubated at 60 °C without shaking in the dark.

For the mesophilic pure culture experimental set (hereafter, MP), we used *Methanobacterium* sp. MO-MB1 isolated from subseafloor sediment in our laboratory (Imachi et al. 2011). The base liquid medium composition for MP was almost the same as that for MC, except that butyrate solution was not added. The MP batches were prepared using almost the same procedure as for the TP batches, except that the headspace gas composition was 160 kPa N_2, 40 kPa CO_2, and 200 kPa H_2. The amount of inoculum for each TP batch was 0.1 mL. Batches of MP were incubated at 30 °C without shaking in the dark.

General notation of isotope ratios

The term "hydrogen" in this paper includes both deuterium (D or ^{2}H) and protium (H or ^{1}H). The relative abundance of D to H or ^{13}C to ^{12}C was noted *R*:

$$R = [\mathrm{D}]/[\mathrm{H}] \text{ or } \left[^{13}\mathrm{C}\right]/\left[^{12}\mathrm{C}\right] \quad (1)$$

We used delta (δ) notation to express the relative difference between the isotope ratio of a sample and a standard in the permil scale:

$$\delta = \left[\left(R_{\mathrm{sample}}/R_{\mathrm{standard}}\right) - 1\right] \times 1000\ (‰). \quad (2)$$

The δD and $\delta^{13}C$ values were calculated with respect to the international standards VSMOW and VPDB, respectively. The isotope fractionation factor, α, is generally defined as the division between the isotope ratios of two molecules as follows:

$$\alpha_{\mathrm{A\text{-}B}} = R_{\mathrm{A}}/R_{\mathrm{B}}, \quad (3)$$

$$\alpha_{\mathrm{A\text{-}B}} = (1000 + \delta_{\mathrm{A}})/(1000 + \delta_{\mathrm{B}}) \quad (4)$$

In this study, each C or H is superscribed with α to indicate carbon or hydrogen isotope fractionation, respectively, for convenience. The fractionation factors at isotopic equilibrium between H_2 – H_2O ($\alpha^{eq}_{H_2-H_2O}$), CH_4 – H_2O ($\alpha^{eq}_{CH_4-H_2O}$), and CH_4 – CO_2 ($\alpha^{eq}_{CH_4-CO_2}$), and their temperature dependency (Bardo and Wolfsberg 1976; Horita and Wesolowski 1994; Horibe and Craig 1995; Horita 2001) are used.

Experimental settings of isotope ratios

To investigate the hydrogen isotope systematics during methanogen growth, the initial δDH_2O and δDH_2 values in the batch cultures were adjusted by adding D_2O and DH molecules (Table 2). For the coculture experiments, the initial δD_{H_2O} values were adjusted to three levels: nonD_2O-labeled (−62‰ to −58‰), moderately D_2O-labeled (+1406‰ to +1639‰), and highly D_2O-labeled (+3286‰ to +3787‰) (see the next section Sampling and analyses for δDH_2O determination). When the H_2–H_2O equilibrium is attained with these δD_{H_2O} values, the equilibrated δD_{H_2} values ($\delta D^{eq}_{H_2}$) will be −755‰ to −709‰ (nonD_2O-labeled), −369‰ to −189‰ (moderately D_2O-labeled), and +120‰ to +479‰ (highly D_2O-labeled) (see Additional file 2), which are calculated from the temperature-dependent $\alpha^{eq}_{H_2-H_2O}$ values (0.309 and 0.260 at 55 °C and 25 °C: Horibe and Craig 1995). Duplicate batches were examined for each of the δD_{H_2O} levels in both coculture experiments (batches A1–A6 for TC and batches B1–B6 for MC). Precultures of the coculture experiments were conducted using the same medium in terms of δD_{H_2O} levels in order to reduce carry-over δD signatures from the precultures.

For the pure culture experiments, the initial δD_{H_2O} values were also adjusted to three levels: nonD_2O-labeled (−59‰ to −43‰), moderately D_2O-labeled (δD_{H_2O} = +1097‰ to +1427‰), and highly D_2O-labeled (δD_{H_2O} = +2317‰ to +3142‰). In addition, the initial δD_{H_2} values were adjusted with respect to the theoretical δD_{H_2} values expected from the H_2–H_2O equilibrium, i.e., we prepared initial δD_{H_2} values that were higher (DH-rich), lower (D_2O-rich), or almost identical to the equilibrated δD_{H_2} value at the incubation temperatures

Table 2 Initial stable hydrogen isotopic conditions for the hydrogenotrophic methanogenesis experiments

Batches	Isotope labeling		Initial value		$\delta^{eq}D_{H_2-H_2O}$
	D_2O	DH	δD_{H_2O}	δD_{H_2}	
Thermophilic coculture experimental set (TC, at 55 °C)					
A1	–	–	−58	–	–
A2	–	–	−62	–	–
A3	+	–	+1624	–	–
A4	+	–	+1639	–	–
A5	++	–	+3771	–	–
A6	++	–	+3787	–	–
Mesophilic coculture experimental set (MC, at 25 °C)					
B1	–	–	−62	–	–
B2	–	–	−58	–	–
B3	+	–	+1406	–	–
B4	+	–	+1413	–	–
B5	++	–	+3662	–	–
B6	++	–	+3286	–	–
Thermophilic pure culture experimental set (TP, at 60 °C)					
C1	–	–	−59	−358	DH-rich
C2	–	+	−53	+330	DH-rich
C3	+	–	+1097	−287	Equilibrated
C4	+	++	+1210	+1886	DH-rich
C5	++	–	+2574	−350	D_2O-rich
C6	++	+	+2317	+70	Equilibrated
Mesophilic pure culture experimental set (MP, at 30 °C)					
D1	–	–	−54	−344	DH-rich
D2	+	+	+1427	+145	DH-rich
D3	+	+	+1424	+22	DH-rich
D4	+	–	+1369	−350	Equilibrated
D5	+	–	+1382	−349	Equilibrated
D6	++	–	+3096	−351	D_2O-rich
D7	++	+	+3142	+85	Equilibrated

(Table 2). Moreover, we predicted that the initial δDH_2 value of the batch during methanogen growth would approach a δD_{H_2} value isotopically equilibrated with the medium H_2O (Valentine et al. 2004; Kawagucci et al. 2014) because it is known that the functions of hydrogenases promote isotope exchange (Vignais 2005; Campbell et al. 2009; Yang et al. 2012; Walter et al. 2012). Six batches for TP (C1–C6) and seven batches for MP (D1–D7) were examined (Table 2). In the same manner as the coculture experiments, precultures for the pure culture experiments were conducted with media containing the same δD_{H_2O} and δD_{H_2} levels in order to reduce carry-over δD signatures from the precultures.

Sampling and analyses

To determine the partial pressures (pH_2 and pCH_4) and isotope ratios (δD_{CH_4}, δD_{H_2}, $\delta^{13}C_{CH_4}$, $\delta^{13}C_{CO_2}$), the headspace gas of each batch was collected during incubation. The sampling frequency was determined on the basis of pCH_4 monitoring in preculture to include both the exponential and stationary growth phases of the methanogens. For the TC and MC, 8 mL of the headspace gas was subsampled into an evacuated 8-mL glass vial at each sampling time to quantify pH_2 and δD_{H_2} at low H_2 level. In contrast, for the TP and MP, 0.5 mL of the headspace gas was subsampled into an 8-mL glass vial filled with ultrapure grade helium (purity is >99.9999 %: Iwatani Gasnetwork Corporation, Osaka, Japan) at 100 kPa for convenience for the isotope ratio analyses. In an attempt to assess the change of δD_{H_2O} during the growth, 2 mL of the medium fluid was collected immediately after the inoculation and at the end of the experiment, filtered with 0.2-μm pore-size filters (ADVANTEC, Tokyo, Japan), and measured within 12 h of sampling. Because of slight changes before and after the incubation (see Additional file 2), we used the δD_{H_2O} value at the end of incubation to evaluate the isotope systematics (Additional file 2). For only TP, cell density was determined using 0.1 mL of medium subsample by a direct cell count with DAPI (4',6-diamidino-2-phenylindole), to evaluate the growth rate and the cell-specific H_2 consumption rate (Kawagucci et al. 2014 and references therein). The cell densities of the other three experimental sets (TC, MC, and MP) could not be determined using this procedure because the cells did not diffuse in the medium but were tightly attached to the surface of the culture bottle.

The partial pressures of H_2 and CH_4 were determined by gas chromatography using a helium ionization detector (GC-HID) with an in-house standard comprising 100 ppm H_2 and CH_4 over a He matrix. Overall errors for pH_2 and pCH_4 analyses were expected to be within 10 %.

The stable hydrogen and carbon isotope ratios for CH_4 were determined by continuous-flow isotope ratio mass spectrometry (CF-IRMS) with an on-line gas preparation and introduction system connected with a mass spectrometer, MAT253 (Thermo Fisher Scientific, Bremen, Germany), based on a previous study (Umezawa et al. 2009). Details of the system and analytical procedure are as follows. A helium-purged purification line made of stainless-steel tubing and including several two-position valves (VICI Precision Sampling, Inc. Louisianna, USA) with chemical and cold traps was used as the on-line gas preparation and introduction system. Ultra-pure-grade helium (purity >99.9999 %: Iwatani Gasnetwork Corporation) was used with further purification by a Molecular Sieve 5A column at −196 °C (liquid-N_2 bath). The sample gas including CH_4 was

introduced via a gas-tight syringe (PRESSURE-LOK® series, VICI Precision Sampling, Inc., Louisiana, USA) into a 30 mL/min (~ + 0.2 MPa) helium stream, named the "precon stream," of the purification line. CH_4 in the sample gas in the precon stream was separated from CO_2 and H_2O by a stainless-steel tubing coil trap held at −110 °C (ethanol/liquid-N_2 bath) and a chemical trap filled with magnesium perchlorate ($Mg(ClO_4)_2$; Merck KGaA, Darmstadt, Germany) and Ascarite II (sodium-hydroxide-coated silica; Thomas Scientific, Swedesboro, New Jersey, USA). Subsequently, CH_4 was condensed on a stainless-steel tubing trap filled with HayeSep-D porous polymer (60/80 mesh, Hayes Separations Inc., Texas, USA) held at −130 °C (ethanol/liquid-N_2 bath) mounted on a two-position six-port valve. After the turn of the valve position to introduce another helium stream set at 1.0 mL/min, named the "GC stream," into the Hayesep-D trap, the condensed CH_4 was released at >80 °C (hot water bath). The CH_4 on the GC stream was again condensed on a capillary trap made of PoraPLOT Q (20 cm long, 0.32 mm i.d.) held at −196 °C (liquid-N_2 bath) for cryofocus and finally released at room temperature. After complete separation of CH_4 from the other molecules by a HP-PLOT Molesieve capillary column (30 m long, 0.32 mm i.d.) at 40 °C, the effluent CH_4 went to the pyrolysis or combustion units (Thermo Fisher Scientific, Massachusetts, USA) to be converted into H_2 or CO_2, respectively. During the analyses, the pyrolysis and combustion units were maintained at 1440 °C and 960 °C, respectively. The pyrolysis unit was conditioned twice a month by repeated injection of 0.2 mL of pure CH_4 to form a graphite coat on the inner wall of the tubing for quantitative conversion of the sample CH_4 to H_2. The CH_4-derived H_2 and CO_2 were finally introduced via an open-split interface, GC Combustion Interface III (Thermo Fisher Scientific, Massachusetts, USA), into MAT253. Hydrogen or carbon isotope ratios were obtained through simultaneous monitoring of H_2^+ isotopologues at $m/z = 2$ and 3 or CO_2^+ isotopologues at $m/z = 44$, 45, and 46, respectively. Stable hydrogen isotope ratio for H_2 was also determined with MAT253 by CF-IRMS in another publication (Kawagucci et al. 2010). Stable carbon isotope ratio for the CO_2 was determined with an isotope-ratio mass spectrometer, DELTA Plus Advantage (Thermo Fisher Scientific), connected to a universal on-line gas preparation and introduction system, GASBENCH II (Thermo Fisher Scientific). Data acquisition for all the IRMS analyses was based on the ISODAT software package (Thermo Fisher Scientific). The amount of H_3^+ ions generated in the ion source, the so-called H_3^+ factor, in the analysis of hydrogen isotope ratios was determined on ISOTAD and was <4.5 (ppm/mV) during the study. The analytical precisions for the $\delta^{13}C_{CO_2}$, $\delta^{13}C_{CH_4}$, δD_{H_2}, and δD_{CH_4} values were estimated by repeated analyses of standard gases to be within 0.5‰, 0.3‰, 10‰, and 5‰, respectively. The determined δ values were calibrated with commercial and/or in-house standard gases as follows: −40.56‰ and −3.57‰ for $\delta^{13}C_{CO_2}$, −74.01‰ and −39.03‰ for $\delta^{13}C_{CH_4}$, −758.22‰ and −11.09‰ for δD_{H_2}, and −185.9‰ for δD_{CH_4}. To minimize analytical errors, amplitudes of ion beams were matched between samples and standards by regulating amounts of the analyses introduced into IRMS. The δD_{H_2O} of the mediums were analyzed using a liquid water isotope analyzer (Los Gatos Research, Inc.) with an analytical precision of 0.5‰. The determined δD_{H_2O} values were calibrated with three commercial standard waters (−154.3‰, −96.4‰, and −9.5‰). Negligible memory effects were confirmed on the analyses that alternated between D-labeled and nonD-labeled samples. For the D-enriched batches, which had δD values far from the calibration ranges (particularly δD_{H_2O}), the analytical accuracy was presumably worse and the calculated $\alpha^{H}_{CH_4-H_2O}$ values from the batches with D-enriched H_2O should be carefully considered.

Results

All the experimental results are illustrated in Fig. 1 and listed in Additional file 2. The results of each experiment are summarized separately below for each culture type.

Results of Thermophilic Coculture (TC)

The pH_2 values of the TC batches were 4.0–6.8 Pa immediately after the inoculation, increased during the early period of growth, and decreased toward the initial level at the later period (Fig. 1a). The highest pH_2 of each TC batch was somewhat different but within the same order of values (28.6–64.9 Pa). The timings of the pH_2 peaks were slightly variable between the batches (5–8 days). Note that the observed pH_2 values were close to the threshold at which hydrogenotrophic methanogens cease H_2 consumption (10^0–10^1 Pa; Lovley 1985; Thauer et al. 2008), suggesting that our experiment covered the lower end of H_2 availability for microbial methanogenesis. The pCH_4 generally showed an exponential increment with the time of growth and reached 5.5–6.2 kPa (Fig. 1b). The increment of pCH_4 accompanied or followed that of pH_2 in each batch (5–8 days). This implies that the growth of hydrogenotrophic methanogens is triggered by the preceding metabolic function (H_2 production) and growth of the hydrogenogenic bacterial counterpart.

The δD_{H_2} values of TC batches were determined only when the pH_2 values were sufficiently high for the δD_{H_2}

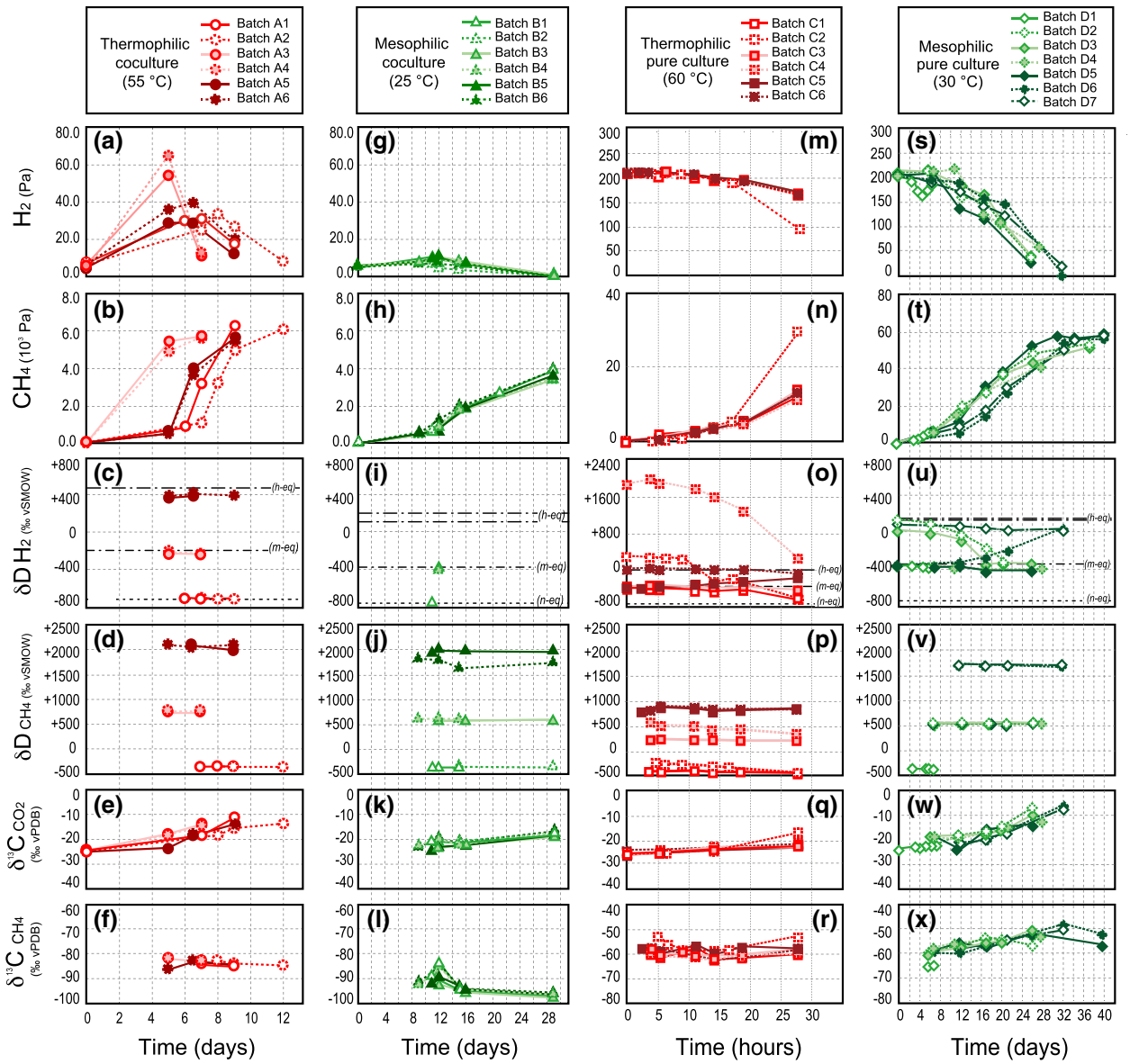

Fig. 1 Temporal changes in H_2, CH_4, and CO_2 in four culture experimental sets. The experimental sets for the thermophilic coculture (**a**–**f**; TC), the mesophilic coculture (**g**–**l**; MC), the thermophilic pure culture (**m**–**r**; TP), and the mesophilic pure culture (**s**–**x**; MP) consisted of experimental batches A1–A6, B1–B6, C1–C6, and D1–D7, respectively. The pH_2 values (panels **a**, **g**, **m**, and **s**), the pCH_4 values (panels **b**, **h**, **n**, and **t**), the δD_{H_2} values (panels **c**, **i**, **o**, and **v**), the δD_{CH_4} values (panels **d**, **j**, **p**, and **v**), the $\delta^{13}C_{CO_2}$ values (panels **e**, **k**, **q**, and **w**), and the $\delta^{13}C_{CH_4}$ values (panels **f**, **l**, **r**, and **x**) were determined for a certain interval of growth from immediately after inoculation to the stationary phase of growth. The symbols are common within each experimental set (TC, MC, TP, and MP)

analysis (pH_2 of >10 Pa) (Fig. 1c). The δD_{H_2} values were virtually identical within batches that had almost identical initial δD_{H_2O} values regardless of pH_2 and time (Fig. 1c). The δD_{H_2} values ranged from −714‰ to −698‰, −231‰ to −213‰, and +374‰ to +413‰ for batches with nonlabeled δD_{H_2O} (A1 and A2), moderately labeled δD_{H_2O} (A3 and A4), and highly labeled δD_{H_2O} (A5 and A6), respectively (Additional file 2). All of these δD_{H_2} values were close to the theoretical δD_{H_2} value at the isotopic equilibrium between H_2 and H_2O ($\delta D^{eq}{}_{H_2}$: see Additional file 2). Our observation is consistent with previous studies examining biologically produced H_2 that also revealed δD_{H_2} values close to the equilibrium (Walter et al. 2012; Yang et al. 2012). Note that the measured δD_{H_2O}–δD_{H_2} relationship showed increased deviation from the theoretically expected relationship in batches with higher δD_{H_2O} values (deviations of <26‰ for A1 and A2, <42‰ for A3 and A4, and <100‰ for A5 and A6). The deviations were beyond the analytical precision of <10‰. Moreover, the deviations were possibly derived from the worse accuracy for the excessively

D-enriched δD_{H_2O} measurement resulting from the over range of calibration by using the commercial standards having relatively lower isotopic values (see Methods) than the δD_{H_2O} values of the experimental batches (Table 2).

The δD_{CH_4} values ranged from −356‰ to −366‰ in A1 and A2, +720‰ to +722‰ in A3 and A4, and +1984‰ to +2092‰ in A5 and A6 (Additional file 2). The δD_{CH_4} values were similar within batches that had similar initial δD_{H_2O} values regardless of pH_2 and time (Fig. 1d); this was also observed for the δD_{H_2} values (Fig. 1c). The $\alpha^{H}_{CH_4-H_2O}$ values calculated from the measured δD_{CH_4} and δD_{H_2O} values were in the ranges 0.673–0.683, 0.655–0.656, and 0.637–0.659 for the nonlabeled, moderately labeled, and highly labeled δD_{H_2O} batches, respectively (Fig. 2 and Additional file 2). There appeared to be a negative correlation between the $\alpha^{H}_{CH_4-H_2O}$ and δD_{H_2O} values. However, when the δD_{H_2O} value calculated from the measured δD_{H_2} value and $\alpha^{eq}_{H_2-H_2O}$ was used instead of the measured δD_{H_2O} value, the resulting $\alpha^{H}_{CH_4-H_2O}$ values fell in a narrower range (0.668–0.697) regardless of the D_2O labels (Fig. 2 and Additional file 2). This $\alpha^{H}_{CH_4-H_2O}$ range is similar to the $\alpha^{H}_{CH_4-H_2O}$ values obtained from the nonlabeled batches using the measured δD_{H_2O} value (0.673–0.683: A1 and A2, Additional file 2). These facts imply that the measured δD_{H_2O} values in the D-enriched batches (e.g., > +1000‰) would be overestimates of the actual values, probably due to the unreliable analytical accuracy in these cases that caused the underestimation of the $\alpha^{H}_{CH_4-H_2O}$ value.

The $\delta^{13}C_{CO_2}$ value for each of the TC batches increased with the time of growth from −23.5‰ to −11.5‰ (Fig. 1e). The $\delta^{13}C_{CH_4}$ values were nearly constant throughout growth, between −86.3‰ and −82.0‰ (Fig. 1f). The resulting $\alpha^{C}_{CH_4-CO_2}$ values generally decreased with time from 0.936 to 0.925 (Fig. 3 and Additional file 2). The $\alpha^{C}_{CH_4-CO_2}$ decreases appeared to be synchronized with the pH_2 decrease (Fig. 4a and Additional file 2), which is harmonious to the pH_2 $-\alpha^{C}_{CH_4-CO_2}$ relationship previously reported (Valentine et al. 2004; Penning et al. 2005; Takai et al. 2008).

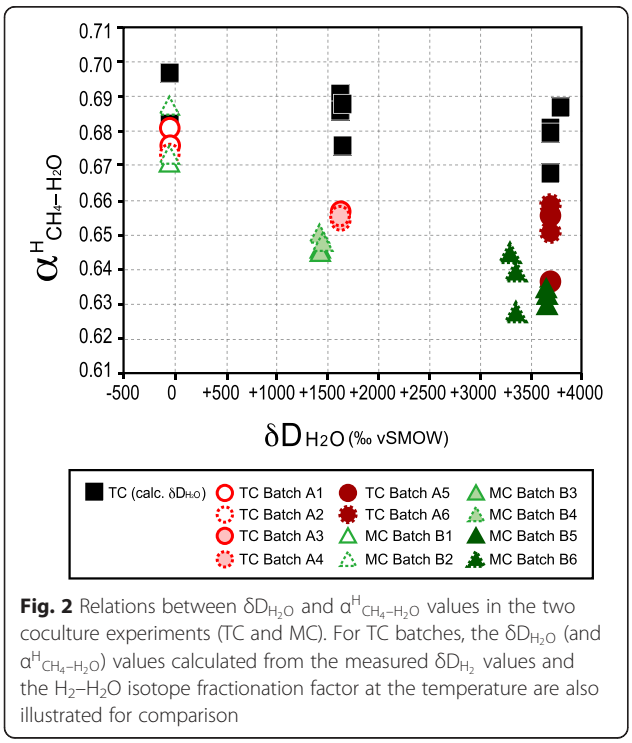

Fig. 2 Relations between δD_{H_2O} and $\alpha^{H}_{CH_4-H_2O}$ values in the two coculture experiments (TC and MC). For TC batches, the δD_{H_2O} (and $\alpha^{H}_{CH_4-H_2O}$) values calculated from the measured δD_{H_2} values and the H_2–H_2O isotope fractionation factor at the temperature are also illustrated for comparison

Results of Mesophilic Cocultures (MC)

The pH_2 values of the MC batches showed trends similar to those of the TC batches: an initial increase during the early phase of growth and a subsequent decrease to the initial level during the later period of growth (Fig. 1g). The highest pH_2 values of each MC batch were 6.8–10.7 Pa, approximately one-fifth lower than those of the TC batches. The pH_2 peaks occurred around 9–12 days after inoculation. The pCH_4 showed an exponential increase after the pH_2 peak and rose to 3.4–3.9 kPa at the end of incubation (29 days, Fig. 1h).

The δD_{H_2} values of MC batches were obtained from only three samples; B1-11 h, B3-12 h, and B4-12 h, because the pH_2 values of the other samples were below the detection limits of δD_{H_2} measurement (Fig. 1i). The δDH_2 values of MC batches (−746‰ for B1-11 h, −357‰ for B3-12 h, and −394‰ for B4-12 h) were similar to those of H_2 isotopically equilibrated with the medium H_2O, as for the TC batches.

The δD_{CH_4} values of the MC batches were virtually identical through the growth in each of the batches except B6 (Fig. 1j). The δD_{CH_4} values ranged from −371‰ to −354‰ in B1 and B2, +560‰ to +589‰ in B3 and B4, +1934‰ to +1959‰ in B5, and +1608 to +1802‰ in B6, whereas reason(s) of the large variation in B6 remain unclear. The measured δD_{CH_4} and δD_{H_2O} values resulted in $\alpha^{H}_{CH_4-H_2O}$ values of 0.671–0.687, 0.645–0.650, and 0.628–0.645 for the nonlabeled, moderately labeled, and highly labeled δD_{H_2O} batches, respectively (Fig. 2 and Additional file 2). As for the TC batches, the MC batches showed a negative correlation between $\alpha^{H}_{CH_4-H_2O}$ and δD_{H_2O} (Fig. 2). The $\alpha^{H}_{CH_4-H_2O}$ values for the nonD_2O-labeled batches were similar between TC and MC (0.673–0.683 and 0.671–0.687, respectively) in spite of the different species, growth temperatures, and pH_2 conditions (Fig. 4b and Additional file 2).

The $\delta^{13}C_{CO_2}$ values of the MC batches increased with the time of growth from −24.7‰ to −17.2‰ (Fig. 1k). The $\delta^{13}C_{CH_4}$ values of the MC batches increased until

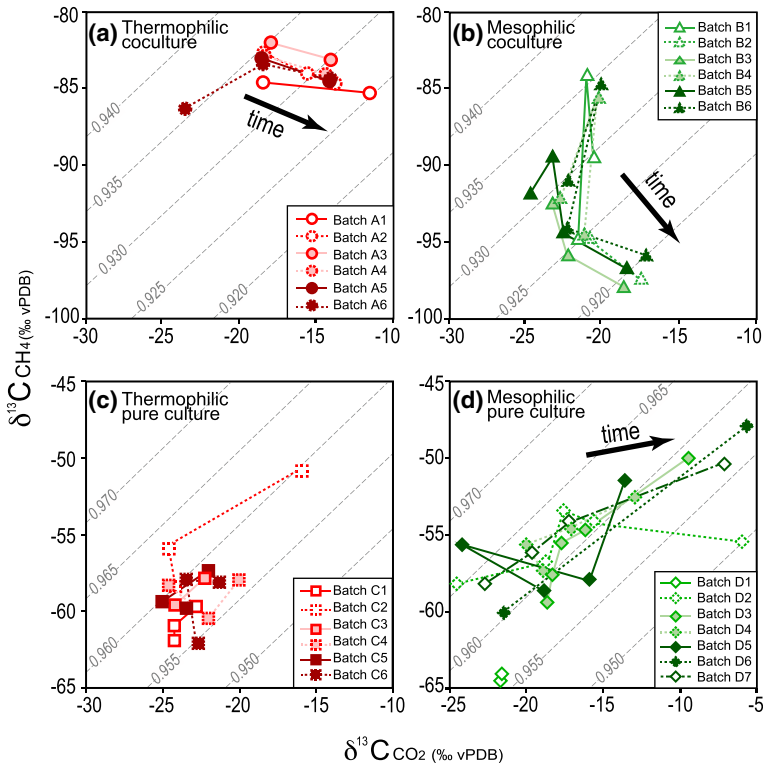

Fig. 3 Relations between $\delta^{13}C_{CO_2}$ and $\delta^{13}C_{CH_4}$ values during growth in each of the four experiment sets (**a**–**d**). Symbols are the same as those in Fig. 1. The black arrow in each panel shows orders of the values along with the time of growth. Diagonal dashed lines indicate the theoretical isotope fractionation factors between CO_2 and CH_4

12 days and subsequently decreased through time. The $\delta^{13}C_{CH4}$ values of the MC batches ranged from −97.9‰ to −84.3‰ (Fig. 1l). The resulting $\alpha^{C}_{CH_4-CO_2}$ values of the MC batches generally decreased through time from 0.935 to 0.919 (Fig. 3b and Additional file 2). The $\alpha^{C}_{CH_4-CO_2}$ range of the MC batches overlapped with but was partly lower than those of the TC batches (Fig. 4a). The last samples of each batch showed the lowest $\alpha^{C}_{CH_4-CO_2}$ values (~0.920) and pH_2 (≤1 Pa), which is harmonious with the positive pH_2-$\alpha^{C}_{CH_4-CO_2}$ relationship.

Results of Thermophilic Pure cultures (TP)

The sampling and analysis for the TP batches were conducted with hourly frequency because of the rapid growth of *Mtc. okinawensis* under high pH_2 conditions (Fig. 1). The pH_2 of the TP batches decreased with time from 210 kPa to 94 kPa for one batch, C2, but to ~160 kPa in the other five batches (Fig. 1m and Additional file 2). The pCH_4 increased exponentially to 30 kPa in batch C2, but to ~12 kPa in the other five batches (Fig. 1n). The H_2 decrement and CH_4 increment roughly matched the stoichiometry in the net reaction of hydrogenotrophic methanogenesis (R1). The cell densities were ~4×10^5 cells/mL at the time of inoculation and exponentially increased to ~5×10^7 cells/mL within 6–15 h in all the batches (Additional file 2). Specific growth rates during the exponential growth phase were estimated to be 0.19 ± 0.05 h^{-1} ($n = 6$). Cell-specific H_2 consumption rates during the exponential growth phase were estimated from the specific growth rate, pCH_4, and the methanogenic stoichiometry (R1) to be 0.14–1.6 fmol-H_2 $cell^{-1}$ s^{-1} ($n = 6$). These values are within cell-specific H_2 consumption rates evaluated in incubation of *Mtb. Thermautotrophicus* under 10^5 Pa-H_2 (0.1–58 fmol-H_2 $cell^{-1}$ s^{-1}), in which the δD_{H_2} effect was exhibited (Kawagucci et al. 2014).

The temporal changes in the δD_{H_2} values showed different directions in the batches that had different initial isotope compositions of H_2 and H_2O (Fig. 1o and Table 2). For the batches that initially had isotopically unequilibrated conditions between H_2 and H_2O (batches C1, C2, C4, and C5), the δD_{H_2} values unidirectionally shifted, either upward or downward, from the initial values toward the equilibrated values (Figs. 5a–c). In the cases of batches that initially had isotopically equilibrated conditions between H_2 and H_2O (batches C3 and C6), the δD_{H_2} values changed little during growth (Fig. 5b and c). The difference between the theoretically expected δD_{H_2} values (equilibrated with δD_{H_2O}) and the

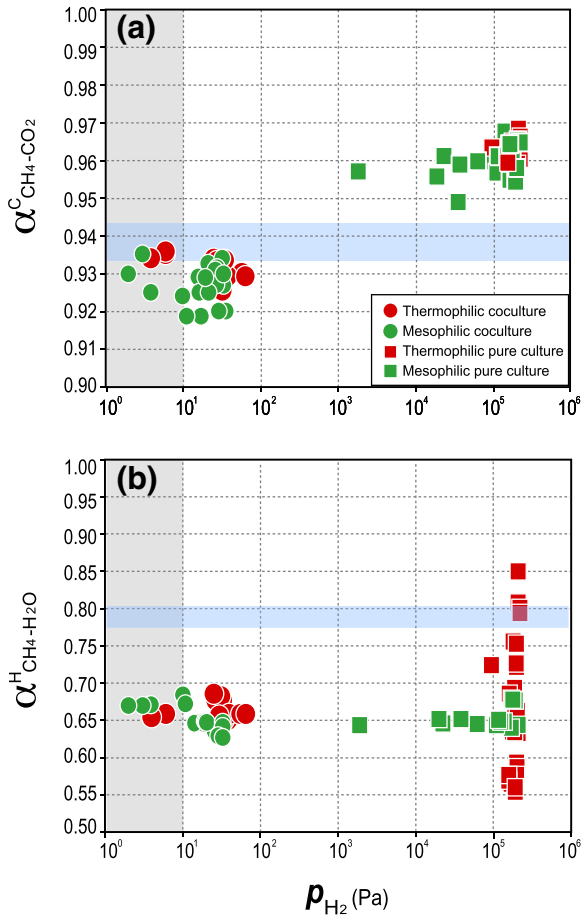

Fig. 4 The isotope fractionations of carbon (**a**) and hydrogen (**b**) with pH_2. The horizontal axis uses a logarithmic scale. Datasets are derived from the thermophilic coculture (TC), the mesophilic coculture (MC), the thermophilic pure culture (TP), and the mesophilic pure culture (MP) in this study

measured δD_{H_2} values of the last samples were within 100‰ except for the batch with the highly DH-labeled H_2 (C4, Table 2) (~600‰).

The δD_{CH_4} values of two batches with highly DH-labeled H_2 (Table 2) decreased with the time of growth from −191‰ to −416‰ in C2 and +585‰ to +360‰ in C4 (Figs. 1p, 5a–c, and Additional file 2). The δD_{CH_4} value of the slightly DH-rich batch (C1) varied in a smaller range (−375‰ to −414‰) than the values of batches C2 and C4. The δD_{CH_4} value of a D_2O-rich batch (C5) and batches C3 and C6 also showed slight changes, which were initially in H_2–H_2O isotopic equilibrium, (Additional file 2). The measured δD_{CH_4} and δD_{H_2O} values resulted in $\alpha^{H}_{CH_4-H_2O}$ values of 0.558–0.850 (Figs. 4b, 5a–c and Additional file 2).

The $\delta^{13}C_{CO_2}$ values for each of the TP batches slightly increased with time of growth from −25.7‰ to −16.8‰ (Fig. 1q and Additional file 2). The $\delta^{13}C_{CH_4}$ values ranged from −62.0‰ to −52.1‰ (Fig. 1r and Additional file 2). The $\alpha^{C}_{CH_4-CO_2}$ values ranged from 0.960 and 0.968 through growth (Fig. 3 and Additional file 2), which were higher than the values of the TC and MC batches (Fig. 4a).

Results of Mesophilic Pure cultures (MP)

The pH_2 values of MP batches decreased with time of growth from ~200 to 1.8–37 kPa (Fig. 1s). The pCH_4 values showed an exponential increase during the early stages of growth and finally plateaued after >30 days of incubation (Fig. 1t). The pCH_4 increment of the MP batches was more than one order of magnitude slower than that of the TP batches. Although the cell-specific H_2 consumption rate cannot be evaluated due to the lack of cell density information, the pCH_4 increment rate implies an H_2 consumption rate that is more than one order of magnitude slower than that of the TP batches (i.e., <~0.1 fmol-H_2 cell^{-1} s^{-1} for MP batches).

Temporal changes of δD_{H_2} values in the MP batches were variable between batches that had different initial isotope compositions of H_2 and H_2O (Fig. 1u and Table 2), as observed in the TP batches. The δD_{H_2} values of batches that initially had isotopically unequilibrated conditions between H_2 and H_2O (D1, D2, D3, and D6) (Table 2) shifted toward the equilibrated values (Fig. 1u). The δD_{H_2} values of batches with initially in isotopic equilibrium between H_2 and H_2O (D4, D5, and D7) showed little change during growth. The differences between the theoretically expected δD_{H_2} values (equilibrated with δD_{H_2O}) and the measured δD_{H_2} values of the last samples were less than 100‰ (Additional file 2).

The δD_{CH_4} values of the MP batches were at around −358‰ in D1, ranged from +536‰ to +581‰ in D2–D5, and were between +1663‰ and +1728‰ in D6 and D7 (Fig. 5d–f and Additional file 2), respectively. The δD_{CH_4} values were highly variable among all the batches but showed small variations between batches that had the same initial δD_{H_2O} values regardless of the time of growth (Fig. 1v). This result suggests that the δD_{CH_4} values depend mostly on the δD_{H_2O} values. The δD_{CH_4} and δD_{H_2O} values resulted in $\alpha^{H}_{CH_4-H_2O}$ values of 0.677–0.679 in D1, 0.647–0.654 in D2–D5, and 0.642–0.657 in D6 and D7 (Fig. 4b and Additional file 2).

The $\delta^{13}C_{CO_2}$ values of the MP batches increased with time of growth from −24.9‰ to −5.7‰ (Fig. 1w). The $\delta^{13}C_{CH_4}$ values also increased from −67.0‰ to −48.0‰ with time (Fig. 1x). The resulting $\alpha^{C}_{CH_4-CO_2}$ values ranged from 0.955 and 0.968 (Fig. 3 and Additional file 2). The $\alpha^{C}_{CH_4-CO_2}$ values in both TP and MP were similar to each other, although the experiments were conducted using different methanogen species with different growth and metabolic kinetics and under different temperature conditions

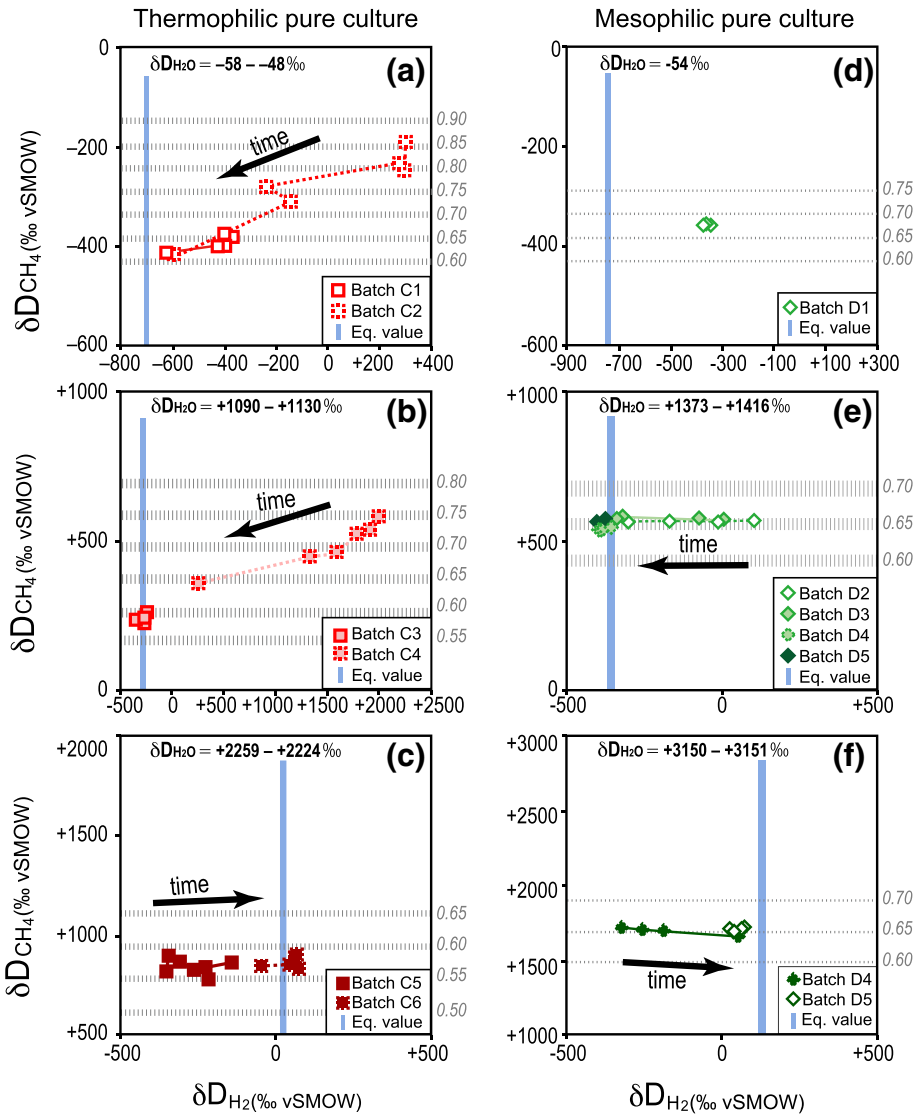

Fig. 5 Relations between δD_{H_2} and δD_{CH_4} in the two pure culture experiment sets (TP and MP). The results were divided into three subsets within each of the experimental sets according to the δD_{H_2O} label conditions: nonD_2O-labeled (panels **a** and **d**); moderately D_2O-labeled (panels **b** and **e**); and highly D_2O-labeled conditions (panels **c** and **f**). The black arrow in each panel marks the trend in the temporal changes of the values. The horizontal dashed lines in each panel indicate the theoretical fractionation factors between CH_4 and H_2O. The vertical gray bar in each panel indicates the equilibrated δD_{H_2} value calculated according to Horibe and Craig (1995)

(Fig. 4a). This result suggests that the stable carbon isotopic fractionation of these hydrogenotrophic methanogens is regulated little with these factors.

Discussion

Carbon isotope fractionation of pure culture and coculture experiments

Comparing the four experimental sets with each other, the $\alpha^{C}_{CH_4-CO_2}$ values were markedly different between the cocultures (0.919–0.936: TC and MC) and the pure cultures (0.949–0.968: TP and MP) (Fig. 4a) in spite of same methanogen used in mesophilic cultures (MC and MP). The $\alpha^{C}_{CH_4-CO_2}$ values in our incubations sometimes overlap but are not always consistent with those at carbon isotope equilibrium (Fig. 4a; 0.933–0.943 at 25–60 °C: Horita 2001). All the $\alpha^{C}_{CH_4-CO_2}$ values obtained in this study (0.919–0.968) fall into the $\alpha^{C}_{CH_4-CO_2}$ range previously determined by experiments between 0.913 (Penning et al. 2005) and 0.989 (Takai et al. 2008) (Fig. 6). The $\alpha^{C}_{CH_4-CO_2}$ values show a positive correlation with the pH_2 condition (Fig. 4a), as determined in previous studies (Valentine et al. 2004; Penning et al. 2005; Takai et al. 2008). These facts allows us to regard the $\alpha^{C}_{CH_4-CO_2}$ value as a proxy for H_2 availability during hydrogenotrophic methanogenesis. As

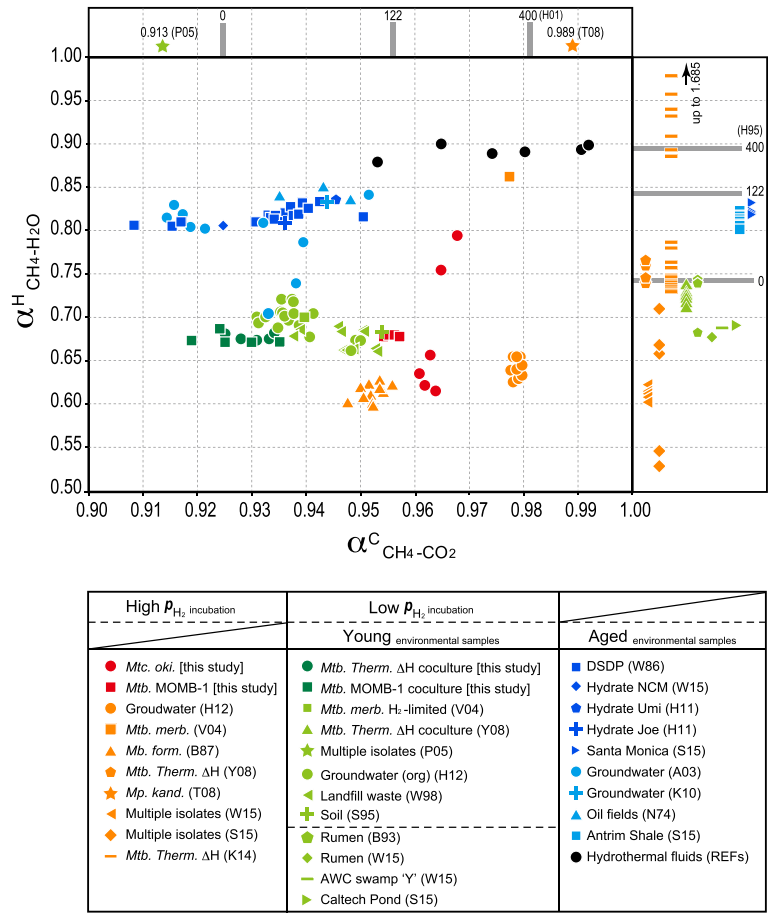

Fig. 6 Compilation of the isotope systematics of hydrogen ($\alpha^{H}_{CH_4-H_2O}$) and carbon ($\alpha^{C}_{CH_4-CO_2}$) associated with in hydrogenotrophic methanogenesis. Symbol colors of reddish, greenish, and bluish respectively represent datasets of laboratory incubations under high pH_2 conditions, incubations under low pH_2 condition and observations of "young" methane reservoirs in nature, and observations of "aged" methane reservoirs. Horizontal and vertical gray bars respectively represent the fractionation factors at the equilibriums of hydrogen ($\alpha^{eq}_{CH_4-H_2O}$) and carbon ($\alpha^{eq}_{CH_4-CO_2}$) at the indicated shown temperatures (0 °C, 122 °C, and 400 °C). All the data sources are listed in the main text (see Discussion)

previous and current incubations examining the $\alpha^{C}_{CH_4-CO_2}$ values have covered a full spectrum of pH_2 conditions from the methanogenic threshold (10^{-1}–10^{1} Pa: e.g., the MC batches in this study) to unrealistic enrichment (10^{7} Pa: Takai et al. 2008), the potential range of $\alpha^{C}_{CH_4-CO_2}$ variation corresponding to pH_2 change has been fully covered.

Hydrogen isotope systematics of syntrophic consortium incubation

The cocultures experiments (TC and MC) exhibited $\alpha^{H}_{CH_4-H_2O}$ values of 0.63–0.69 through the growth phase shift, although the experiments were conducted under different temperatures and with different syntrophic couples (Fig. 6). The $\alpha^{H}_{CH_4-H_2O}$ values of 0.67–0.69 from the nonD_2O-labeled batches represent the most reliable range, as discussed above (Fig. 2). A slightly higher $\alpha^{H}_{CH_4-H_2O}$ range (0.71–0.74) was obtained in previous coculture experiments with the same hydrogenotrophic methanogenic consortium, *S. lipocalidus* and *Mtb. thermautotrophicus* at 55 °C (Yoshioka et al. 2008) (Fig. 6). In addition to these syntrophic consortiums reconstructed in the laboratory, similar $\alpha^{H}_{CH_4-H_2O}$ values have been reported from experiments using potential H_2-syntrophic communities in natural environments such as in soil (0.68) (Sugimoto and Wada 1995), groundwater (0.66–0.73) (Hattori et al. 2012), and landfill waste (0.66–0.69) (Waldron et al. 1998) (Fig. 6). Note that there was considerable variation in $\alpha^{H}_{CH_4-H_2O}$ (0.66–0.74) in these studies compared to the typical analytical errors of δD_{H_2O} and δD_{CH_4} values (≤ ~ 10‰), corresponding to the $\alpha^{H}_{CH_4-H_2O}$ deviation of ≤ ~0.01. The reason why such variation of stable hydrogen isotope fractionation occurs in various potentially H_2-syntrophic communities is currently unknown. The hydrogen

isotope equilibrium at methanogenic temperatures of our culture (0.775–0.809 at 25 °C – 60 °C: Horibe and Craig 1995) does not account for the $\alpha^{H}_{CH_4-H_2O}$ values observed (Fig. 4b). Nevertheless, the $\alpha^{H}_{CH_4-H_2O}$ range of 0.66–0.74 probably represents the potential hydrogen isotopic signature of methane derived from hydrogenotrophic methanogenesis that occurs in H_2-limited habitats at methanogenic rates within the experimental time scale (typically shorter than a year).

Hydrogen isotope systematics of pure culture incubation

Stable hydrogen isotope fractionation in hydrogenotrophic methanogenesis ($\alpha^{H}_{CH_4-H_2O}$) under H_2-enriched conditions (>10^4 Pa-H_2) has been examined using pure cultures of methanogens (Additional file 1): 0.55–0.86 for *Mtb. marburgensis* (Valentine et al. 2004; Stolper et al. 2015); 0.60–1.69 for *Mtb. thermautotrophicus* (Yoshioka et al. 2008; Kawagucci et al. 2014; Wang et al. 2015); 0.528 for *Methanosarcina barkeri* (Stolper et al. 2015); 0.59–0.63 for *Methanobacterium formicicum* (Balabane et al. 1987); 0.64–0.68 for *Methanobacterium* sp. MO-MB1 (MP in this study); and 0.56–0.85 for *Mtc. okinawensis* (TP in this study) (Fig. 6). In addition to the pure cultures, natural groundwater was also incubated with 10^5 Pa-H_2 supply that yielded $\alpha^{H}_{CH_4-H_2O}$ values of 0.63–0.66 (Hattori et al. 2012). The variation of $\alpha^{H}_{CH_4-H_2O}$ values from the H_2-enriched condition (0.55–1.69) is much greater than that from the H_2-limited cultures (0.66–0.74) (Fig. 4b). The high variability of $\alpha^{H}_{CH_4-H_2O}$ values under high pH_2 conditions makes it difficult to estimate the relationship between the $\alpha^{H}_{CH_4-H_2O}$ values and pH_2 conditions during hydrogenotrophic methanogenesis (Burke 1993; Sugimoto and Wada 1995; Valentine et al. 2004; Yoshioka et al. 2008; Hattori et al. 2012; Stolper et al. 2015; Wang et al. 2015). Instead, the large $\alpha^{H}_{CH_4-H_2O}$ variation seems to be regulated by some other factors than pH_2.

One possible factor is the δD_{H_2} effect: the stable isotope signature of the substrate H_2 affects that of the product CH_4 during methane production by rapidly growing hydrogenotrophic methanogens (Kawagucci et al. 2014). In fact, TP batches in this study clearly showed a positive correlation between $\alpha^{H}_{CH_4-H_2O}$ and δD_{H_2} values during the early growth phase (Fig. 5), as also observed in a previous study of *Mtb. thermautotrophicus* (Kawagucci et al. 2014). In addition, the δD_{H_2} effect has been detected during reexamination of experimental datasets published in the literatures. For example, the $\alpha^{H}_{CH_4-H_2O}$ variation was observed during the growth of *Mtb. marburgensis* in a flow-through culture fed with D-enriched H_2 (δD_{H_2} = −187‰) and slightly D-depleted H_2O (δD_{H_2O} = −93‰), and the highest $\alpha^{H}_{CH_4-H_2O}$ value of 0.86 was obtained from the early growth phase (Valentine et al. 2004). The lowermost $\alpha^{H}_{CH_4-H_2O}$ value of 0.59 was obtained during the growth of *Mtb. formicicum* in a batch culture fed with D-depleted H_2 (δD_{H_2} = −728‰) and slightly D-enriched H_2O (δD_{H_2O} = +39‰) (Balabane et al. 1987). These results suggest that the δD_{H_2} effect may have a significant impact on the $\alpha^{H}_{CH_4-H_2O}$ values under high pH_2 conditions. The δD_{H_2} effect potentially leads to a great variation of $\alpha^{H}_{CH_4-H_2O}$ values as a result of the contribution from δD_{H_2} variation.

In contrast, it was notable that little δD_{H_2} effect was exhibited in MP batches, which cultivated a hydrogenotrophic methanogen under high pH_2 conditions (Fig. 5a–c). This finding implies that the δD_{H_2} effect is not directly associated with the pH_2 conditions of growth. The hydrogen isotope fractionation in hydrogenotrophic methanogenesis is thought to be related to the methanogenic rate (Valentine et al. 2004; Stolper et al. 2015). As the MP batches reached the stationary growth phase after several weeks, which is slower than the typical growth rates of other pure culture methanogens at >10^4 Pa-H_2 with favorable growth conditions (timescales of hours to days: Additional file 1), the δDH_2 effect may instead be related to the metabolic and growth kinetics of methanogens.

As discussed in previous studies (Burke 1993; Sugimoto and Wada 1995; Kawagucci et al. 2014), the incorporation of intracellularly produced H^+ from the H_2 into CH_4 may drive the δD_{H_2} effect. From this viewpoint, a previous study that cultivated *Mtb. thermautotrophicus* under high-pH_2 conditions attempted to yield a quantitative understanding of the magnitude of the δD_{H_2} effect (Kawagucci et al. 2014). We can know only two quantitative pieces of information relating to the δD_{H_2} effect: the cell-specific H_2 consumption rate (i.e., the intracellular H^+ production rate) of 10^{-1}–10^2 fmol/cell/s and the quantity of intracellular H_2O, which is 10^1–10^2 fmol-H_2O. If the H_2 consumption rate is comparable with that trans-membrane H_2O and H^+ flux, which remains unknown, the intracellular δD_{H_2O} value should be affected by H_2-derived H_2O (H^+) that results in exhibition of the δD_{H_2} effect. Moreover, if the trans-membrane H_2O flux is constant regardless of the cell growth situation, the slower H_2 consumption rate would lead to a smaller δD_{H_2} effect. It would be reasonable for a significant δD_{H_2} effect to be apparent in the TP batches and *Mtb. thermautotrophicus* batches reported previously (Kawagucci et al. 2014), in which the H_2 consumption rate was rapid (10^{-1}–10^2 fmol/cell/s), whereas little δD_{H_2} effect was detected in the MP batches, in which the H_2 consumption rate was slow (presumably < ~10^{-1} fmol/cell/s). This finding seems consistent with the decrement in magnitude of the δD_{H_2} effect along with the growth phase shift from exponential growth to the stationary phase (Kawagucci et al. 2014).

Comparison between methanogenic experiments and environmental methane

To compare the experimental results with natural environments, we here review hydrogen and carbon isotope fractionations that have been obtained from environmental observations in addition to the incubations (Additional file 1). As the timescale of methanogenesis is a probable key factor controlling hydrogen isotope fractionation, as aforementioned, the compiled dataset of natural isotope fractionations is classified by considering the timescales of natural methane reservoirs (Fig. 6). Methane in the bovine rumen, one of the natural environments in which methane generation occurs as rapidly as in laboratory incubations, showed the $\alpha^{H}_{CH_4-H_2O}$ range between 0.68 and 0.74 (Burke 1993; Wang et al. 2015). The pH_2 condition of the rumen was estimated at ~10^2 Pa (Burke 1993; Wang et al. 2015), higher than the values exhibited in our cocultures (<65 Pa: Fig. 1) and the methanogenic threshold (<10^1 Pa: Lovley 1985; Thauer et al. 2008). Terrestrial sediments in freshwater systems of Caltech pond and Swamp Y (Stolper et al. 2015; Wang et al. 2015) possessed $\alpha^{H}_{CH_4-H_2O}$ values of ~0.69. The $\alpha^{H}_{CH_4-H_2O}$ values in these environmental samples from relatively "young" methane reservoirs (0.68–0.74) are consistent with those obtained from the regulated laboratory cocultures of hydrogenotrophic methanogens (≤0.74). Note that aceticlastic and/or methylotrophic methanogenesis may also occur in the wild environment.

Hydrogen and carbon isotope fractionations have also been investigated in geological methane reservoirs: natural gas fields (Nakai et al. 1974; Whiticar et al. 1986); continental groundwater at the Elk Valley coalbed methane field (Aravena et al. 2003); terrestrial groundwater associated with the accretionary prism in south-east Japan (Kimura et al. 2010); deep-sea sediments (Whiticar et al. 1986); and subseafloor methane hydrate deposits from the Northern Cascadia Margin (Wang et al. 2015), the Umitaka Spur, and the Joetsu Knoll of the Japan Sea (Hachikubo et al. 2011) (Fig. 6). We hereafter methane in geological reservoirs is named as "aged" methane, for comparison with "young" methane in laboratory cultures and natural environments, as aforementioned. Almost all of these aged samples show a $\alpha^{C}_{CH_4-CO_2}$ range of 0.91–0.95, suggesting that hydrogenotrophic methanogenesis under H_2-limited conditions is plausible as the geochemical origin of these methane. Almost all of the $\alpha^{H}_{CH_4-H_2O}$ values of the aged methane samples fall within a narrow range of 0.79–0.84 (Fig. 6). The $\alpha^{H}_{CH_4-H_2O}$ values are not consistent with the values obtained from the H_2-limited experiments and young environmental samples (≤0.74; Fig. 6) in spite of the commonly low $\alpha^{C}_{CH_4-CO_2}$ values (≤0.95).

Possible mechanisms exhibiting variable isotope fractionation

We define three major provinces in the compilation of isotope fractionations (Fig. 6) and infer the metabolic mechanisms functioning to yield each of the provinces as follows (Fig. 7). The first province has an $\alpha^{C}_{CH_4-CO_2}$ range higher than 0.95 with highly variable $\alpha^{H}_{CH_4-H_2O}$ values (Fig. 6). This province has occurred in >10^4 Pa-H_2 culture but never observed in any natural samples from biologically functionable temperature environments (≤122 °C). This finding is reasonable because such high-pH_2 environments are rare in nature, except for several H_2-enriched geofluid systems (Charlou et al. 2002; Proskurowski et al. 2006; Ishibashi et al. 2014). The high $\alpha^{C}_{CH_4-CO_2}$ value in >10^4 Pa-H_2 cultures has been thought to be a result of an almost straightforward progress of carbon reduction from CO_2 to CH_4 in a multistep methanogenic pathway (Valentine et al. 2004; Penning et al. 2005; Fig. 7a and b). The large $\alpha^{H}_{CH_4-H_2O}$ variation probably results from the δD_{H_2} effect (see discussion above), and the magnitude of the δD_{H_2} effect appears to be linked to the H_2 consumption rate (Fig. 7a and b). The δD_{H_2} shift, probably due to H_2–H_2O isotope exchange toward the isotope equilibrium by reversible function of hydrogenase, suggests that H_2 reproduction functioned even during the almost straightforward methanogenesis (Fig. 7b).

The second province has an $\alpha^{C}_{CH_4-CO_2}$ range lower than 0.95 and an $\alpha^{H}_{CH_4-H_2O}$ range of 0.67–0.74 (Fig. 6). This province has been found in both laboratory cultures of <10^4 Pa-H_2 conditions and also in natural reservoirs of relatively young methane such as the bovine rumen and terrestrial sediments. The low $\alpha^{C}_{CH_4-CO_2}$ values are thought to result from the extent of reversibility of the methanogenic pathway under low-pH_2 conditions (Valentine et al. 2004; Fig. 7c). The narrow $\alpha^{H}_{CH_4-H_2O}$ range is probably caused by a combination of the higher reversibility and the slower H_2 consumption rate. The slow H_2 consumption would alter the intracellular δD_{H_2O} value little and leave it the same as the environmental (extracellular) δD_{H_2O} value (Fig. 7c). The repeated formation and cleavage of the C–H bonds of methane precursors through the reversible methanogenic pathway lead to hydrogen isotope equilibrium between the precursor and intracellular water. Note that the $\alpha^{H}_{CH_4-H_2O}$ values of this province (0.67–0.74) are out of the $\alpha^{eq}_{CH_4-H_2O}$ range between 0 °C and 400 °C (Horibe and Craig 1995). This finding suggests that some kinetic processes are also involved in the hydrogen isotope fractionation (Fig. 7c).

The third province has an $\alpha^{C}_{CH_4-CO_2}$ range lower than 0.95 and an $\alpha^{H}_{CH_4-H_2O}$ range higher than 0.80 (Fig. 6). The third province overlaps with the second

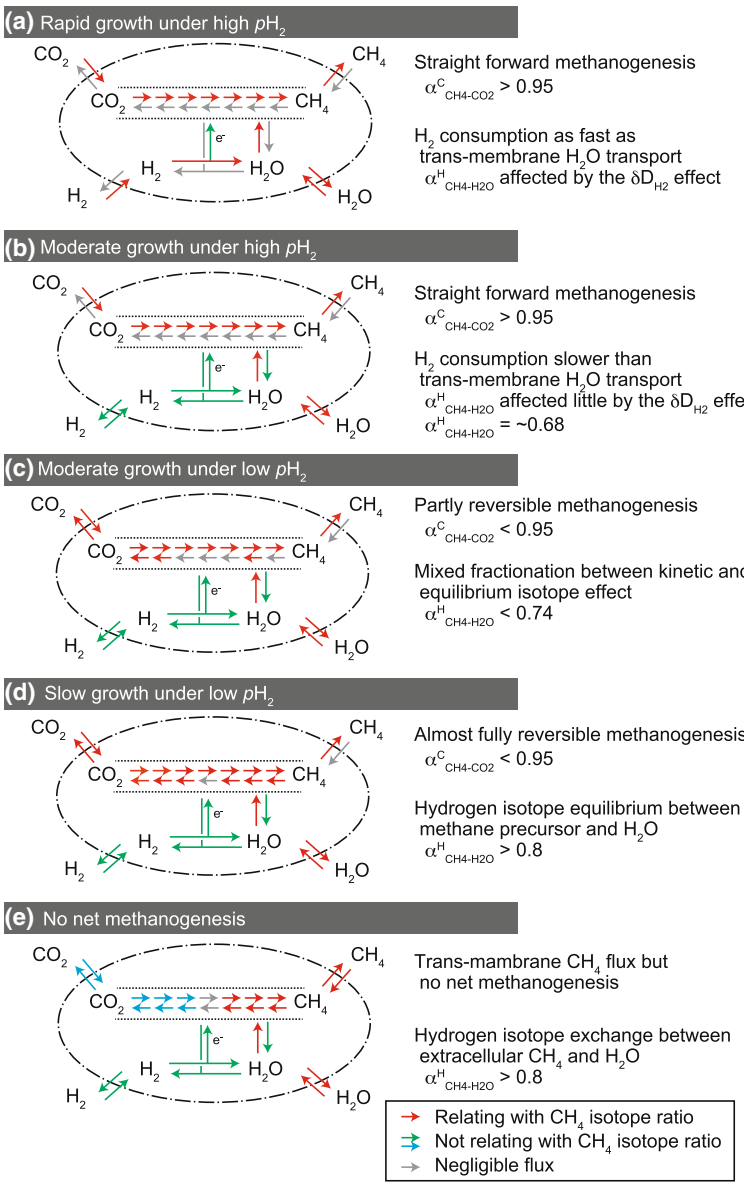

Fig. 7 Cartoons of intra- and trans-membrane fluxes of the molecules in hydrogenotrophic methanogenesis relating to hydrogen and carbon isotope systematics. Each five panel represents methanogenic characteristics with respect to growth rate and pH_2 condition for the growth. Red arrows represent significant molecular fluxes relating with CH_4 isotope ratios. Light green and blue arrows represent significant molecular fluxes not relating with CH_4 isotope ratios. Grey arrows represent negligible molecular fluxes. Dash-dotted circles are cell membrane, and arrows enclosed by dotted lines represent multistep methanogenic reaction (numbers of the arrows have no meaning). A term "H_2O" in cartoon represents both H_2O and H^+. See main text for details

province in $\alpha^{C}_{CH_4-CO_2}$ values but differs in the $\alpha^{H}_{CH_4-H_2O}$ value. This province has been observed typically in geological reservoirs of aged methane such as natural gas and seafloor methane hydrate. It was thought that methanogenesis at an extremely slow rate could produce the third province because of isotopic equilibrium between H_2O, H_2, CO_2, and methane precursors through a highly reversible methanogenic pathway (Stolper et al. 2015; Wang et al. 2015; Fig. 7d). Unfortunately, we cannot examine this possibility experimentally because microbial methanogenesis at a rate as slow as geological timescale is not reproducible by experiments. In addition, we are aware of the $\alpha^{C}_{CH_4-CO_2}$ variation in spite of the narrow $\alpha^{H}_{CH_4-H_2O}$ range within the third province (Fig. 6). The $\alpha^{C}_{CH_4-CO_2}$ variation may be inconsistent with this explanation because methanogenesis

through the geological timescale is expected to occur under constantly low pH_2 conditions and slow growth rate, resulting in the constantly low $\alpha^{C}_{CH_4-CO_2}$ value of approximately 0.92.

We here hypothesize that the higher $\alpha^{H}_{CH_4-H_2O}$ values of the third province may be caused by a post-methanogenesis process over geological timescales (Fig. 7e) rather than the methanogenesis through geological timescale (Fig. 7d). This process is diagenetic hydrogen isotope exchange between extracellular CH_4 and H_2O promoted by the reversible function of the multistep methanogenic pathway in methanogenic region and/or methane reservoirs after the migration (Fig. 7e). Multiple lines of circumstantial evidence based on biological and geochemical viewpoints can be cited to put forward the possibility of the diagenetic hydrogen isotope exchange as following. First, the microbial methanogenic pathway is also able to operate reversibly for methane consumption; e.g., it is known that anaerobic methanotrophic archaea can oxidize CH_4 via potential reverse methanogenesis (Knittel and Boetius 2009) and the methanogens can perform trace methane oxidation even during active methanogenesis (Moran et al. 2005). In addition, trans-membrane exchange of CH_4 would be not negligible in geological timescale. Thus, the reversible enzymatic reactions, in particular at the later steps of the methanogenesis, i.e., cleavage and reproduction of C–H bonds of CH_4, could result in promoting the hydrogen isotope exchange between extracellular CH_4 and H_2O (Fig. 7e). Second, the $\alpha^{H}_{CH_4-H_2O}$ values in the third province (0.79–0.86) overlap with the $\alpha^{eq}_{CH_4-H_2O}$ values in the known biologically-functional temperature range (0.758–0.843 at 0–122 °C: Horibe and Craig 1995) (Fig. 6). Third, a one-year hydrothermal experiment at 323 °C (Reeves et al. 2012) revealed negligible hydrogen isotope exchange between CH_4 and H_2O. This finding suggests that hydrogen isotope exchange is extremely sluggish in the habitable temperature range without effective catalysts such as enzymes in the reversible methanogenic pathway. Fourth, the third province is only detected in the aged methane samples obtained from both marine and terrestrial environments (Fig. 6) while relatively young methane samples such as from the rumen and laboratory experiments are never located in the third province. This age-isotope relationship is also found in a "clumped" isotope composition, i.e., the abundance of ^{13}C–D bonds in CH_4, which may yield information about the temperature at which the C–H bonds were formed or last equilibrated (Stolper et al. 2014, 2015; Ono et al. 2014; Wang et al. 2015). The clumped isotope composition so far observed in aged methane reservoirs indicates the CH_4–H_2O equilibrated signature, whereas clumped signatures that cannot be explained by expected formation temperature have been found frequently in young biogenic methane from natural reservoirs and laboratory incubations (Stolper et al. 2014, 2015; Wang et al. 2015). Fifth, the diagenetic hydrogen isotope exchange is not in conflict with the broad $\alpha^{C}_{CH_4-CO_2}$ range of the third province. If a methane reservoir incorporates multiple methane sources, each of which has distinct isotope signatures, the diagenetic hydrogen isotope exchange could unify the $\alpha^{H}_{CH_4-H_2O}$ values regardless of the sources but leave the $\alpha^{C}_{CH_4-CO_2}$ value as a mixed signature because of incomplete molecular equilibrium between CO_2 and CH_4 (Fig. 7e). Such diagenetic unification of the hydrogen isotope ratio while maintaining the $\alpha^{C}_{CH_4-CO_2}$ variation is evident in deep-sea, high-temperature hydrothermal fluids (Fig. 6: Proskurowski et al. 2006; McCollom 2008; Kawagucci et al. 2013a; 2013b; Wang et al. 2015). Methane in the hydrothermal fluids so far observed in various geological settings shows a broad $\alpha^{C}_{CH_4-CO_2}$ range (0.953–0.992) but a narrow $\alpha^{H}_{CH_4-H_2O}$ range (0.88–0.90), which are close to the $\alpha^{eq}_{CH_4-H_2O}$ values at the endmember fluid temperatures (~0.87 at 300 °C–400 °C: Horibe and Craig 1995).

These pieces of circumstantial evidence put forward that the hydrogen isotope signature of CH_4 imprinted at the time of hydrogenotrophic methanogenesis ($\alpha^{H}_{CH_4-H_2O} = 0.66–0.74$), belonging to second province, can be altered by the reversible reactions of the multistep methanogenic pathway, which leads to CH_4–H_2O isotopic equilibrium at habitable temperatures ($\alpha^{H}_{CH_4-H_2O} > 0.76$) belonging to the third province. If this is true, the hydrogen isotope ratio of methane in geological samples would be useless as a tracer to deduce the origin of methane. However, it is also possible to criticize this hypothesis: the diagenetic isotope exchange proposed here is not required when methanogenesis through geological time actually exhibits isotope fractionation in the third province, as aforementioned. Furthermore, an in vitro biochemical study of methyl coenzyme M reductase activity, which is an enzyme that catalyzes the last step of methanogenesis, showed that little hydrogen isotope exchange between CH_4 and H_2O occurred during the enzyme reaction for several tens of minutes (Scheller et al. 2013). It is still uncertain whether diagenetic hydrogen isotope exchange can be promoted by methanogens or not and how rapid the isotope exchange is if it occurs. To solve these uncertainties, experiments using methanogenic cells concentrated in mediums with isotopically disequilibrated CH_4 and H_2O under thermodynamic states favorable to each of methane generation and methane consumption will be conducted.

That work will provide experimental justification of the possible post-methanogenesis isotope diagenesis hypothesis.

Conclusions

This study confirmed five facts as follows.

1. Carbon isotope fractionation between CH_4 and CO_2 during hydrogenotrophic methanogenesis is correlated with pH_2, as suggested in previous studies (Valentine et al. 2004; Penning et al. 2005; Takai et al. 2008).
2. The hydrogen isotope ratio of CH_4 produced by a thermophilic methanogen, *Mtc. okinawensis*, under high pH_2 conditions (~10^5 Pa-H_2) is affected by the isotope ratio of H_2, as pointed out in a previous incubation of *Mtb. thermautotrophicus* (Kawagucci et al. 2014). This pattern is named as the δD_{H_2} effect. This effect also appears to account for the diverse hydrogen isotope fractionation between CH_4 and H_2O previously observed in H_2-enriched culture incubations (Balabane et al. 1987; Valentine et al. 2004; Stolper et al. 2015; Wang et al. 2015).
3. A mesophilic methanogen, *Methanobacterium* sp. MO-MB1, showed little δD_{H_2} effect even under high-pH_2 conditions (~10^5 Pa). This result suggests that methanogenic and growth rates rather than the pH_2 condition are significant factors controlling the δD_{H_2} effect.
4. The hydrogen isotope fractionation between CH_4 and H_2O in hydrogenotrophic methanogenesis under low pH_2 conditions (<10^2 Pa) observed in experiments is in the range of 0.66–0.74.
5. Hydrogen isotope fractionation exhibited in laboratory incubations under low-pH_2 conditions is consistent with that observed in "young" methane reservoirs but inconsistent with that observed in "aged" methane reservoirs.

In conclusion, we propose that diagenetic hydrogen isotope exchange between extracellular CH_4 and H_2O catalyzed by a reversible methanogenic pathway of methanogenic populations alters the hydrogen isotope signature of CH_4 imprinted at the time of generation.

Additional files

Additional file 1: Compilation of hydrogen and carbon isotope systematics from incubation and observation. Description of data: Type of ecosystem, name of ecosystem, temperature of methanogen growth (Celsius), approximate timescale for growth, fractionation factors of the carbon isotope ratio between CH_4 and CO_2 ($\alpha^{C}_{CH_4-CO_2}$), fractionation factors of the hydrogen isotope ratio between CH_4 and H_2O ($\alpha^{H}_{CH_4-H_2O}$), and references. (XLSX 53 kb)

Additional file 2: All results. Description of data: Batch culture names, sampling times (h; hours or d; days), hydrogen concentration (Pa), methane concentration (kPa), hydrogen isotope ratio of H_2O, H_2, and CH_4 (‰ vs. VSMOW), carbon isotope ratio of CO_2 and CH_4 (‰ vs. VPDB), values of equilibrated hydrogen isotope ratio of H_2 ($\delta^{eq}D_{H_2}$) between H_2 and H_2O, fractionation factors of the carbon isotope ratio between CH_4 and CO_2 ($\alpha^{C}_{CH_4-CO_2}$), and fractionation factors of the hydrogen isotope ratio between CH_4 and H_2O ($\alpha^{H}_{CH_4-H_2O}$). Cell numbers were counted only in the thermophilic pure culture batches. (XLSX 58 kb)

Abbreviations

CF-IRMS: continuous-flow isotope ratio mass spectrometry; DSMZ: Deutsche Sammlung von Mikroorganismen und Zellkulturen; Eq: isotope equilibrium; GC-HID: gas chromatography using a helium ionization detector; MC: Mesophilic coculture experimental set; MP: Mesophilic pure culture experimental set; Mtb: *Methanothermobacter*; *Mtc*: *Methanothermococcus*; *S*: *Syntrophothermus*; TC: Thermophilic coculture experimental set; TP: Thermophilic pure culture experimental set; VPDB: Vienna Pee Dee Belemnite; VSMOW: Vienna standard mean ocean water.

Competing interests

The authors declared that they have no competing interests.

Authors' contributions

SK proposed the topic, conceived, and designed the study. TO performed all the experiments and measurements. YS and HI contributed to incubation and interpretation of the TC, MC, and MP experiments. YM analyzed the carbon isotopes of CO_2 and CH_4 and assisted with their interpretation. TO and SK compiled the results and drafted the manuscript. KT collaborated with the corresponding author in the design of the study and the construction of the manuscript. All authors read and approved the final manuscript.

Authors' information

TO is a JSPS research fellow for young scientist adopted at the Laboratory of Ocean-Earth Life Evolution Research (OELE), Japan Agency for Marine-Earth Scienceand Technology (JAMSTEC). SK is a researcher at OELE, Department of Subsurface Geobiological Analysis and Research (D-SUGAR), and Research and Development (R&D) Center for Submarine Resources, JAMSTEC. During this study, YS was a graduate school student at the Department of Environmental Systems Engineering, Nagaoka University of Technology. HI is a senior researcher at the D-SUGAR and R&D Center for Submarine Resources, JAMSTEC. YM is an engineer at the R&D Center for Submarine Resources, JAMSTEC. KT is a principal scientist at D-SUGAR, OELE, and the R&D Center for Submarine Resources, JAMSTEC.

Acknowledgements

We wish to thank Uta Konno, Keiko Tanaka, Eiji Tasumi, and Sanae Sakai for their assistance on microbial incubation and chemical analysis. The authors would like to thank Enago (www.enago.jp) for the English language review. Funds for this project were partly provided by the Ministry of Education, Culture, Sports, Science, and Technology, Japan as Grant-in-aids for Young Scientists (A) (25701004 and 15H05468), Scientific Research (A) (15H02419), Scientific Research (C) (22560811), and the JSPS research fellowship for young scientist (26–10363). This project was also supported by Cross-Ministerial Strategic Innovation promotion Program, organized by the Cabinet Office of Japan, for the Development of New-Generation Research Protocol for Submarine Resources.

Author details

[1]Laboratory of Ocean-Earth Life Evolution Research (OELE), Japan Agency for Marine-Earth Science and Technology (JAMSTEC), 2-15 Natsushima-cho, Yokosuka 237-0061, Japan. [2]Department of Subsurface Geobiological Analysis and Research (D-SUGAR), Japan Agency for Marine-Earth Science and Technology (JAMSTEC), 2-15 Natsushima-cho, Yokosuka 237-0061, Japan. [3]Research and Development Center for Submarine Resources, Japan Agency for Marine-Earth Science and Technology (JAMSTEC), 2-15 Natsushima-cho, Yokosuka 237-0061, Japan. [4]Department of Environmental Systems Engineering, Nagaoka University of Technology, 1603-1 Kamitomiokamachi, Nagaoka 940-2188, Japan.

Received: 15 November 2015 Accepted: 18 April 2016
Published online: 12 May 2016

References

Aravena R, Harrison SM, Abercrombie H, Rudolph D (2003) Origin of methane in the Elk Valley coalfield, southeastern British Columbia, Canada. Chem Geol 195:219–227

Balabane M, Galimov E, Hermann M, Letolle R (1987) Hydrogen and carbon isotope fractionation during experimental production of bacterial methane. Org Geochem 11:115–119

Bardo RD, Wolfsberg M (1976) A theoretical calculation of the equilibrium constant for the isotopic exchange reaction between H_2O and HD. J Physic Chem 80:1068–1071

Burke RA (1993) Possible influence of hydrogen concentration on microbial methane stable hydrogen isotopic composition. Chemosph 26:55–67

Campbell BJ, Li C, Sessions AL, Valentine DL (2009) Hydrogen isotopic fractionation in lipid biosynthesis by H_2-consuming *Desulfobacterium autotrophicum*. Geochim Cosmochim Acta 73:2744–2757

Charlou JL, Donval JP, Fouquet Y, Jean-Baptiste P, Holm N (2002) Geochemistry of high H2 and CH4 vent fluids issuing from ultramafic rocks at the Rainbow hydrothermal field (36°14′N, MAR). Chem Geol 191:345–359

Daniels L, Fulton G, Spencer RW, Ormejohnson WH (1980) Origin of hydrogen in methane produced by *Methanobacterium Thermoautotrophicum*. J Bacteriol 141:694–698

Hachikubo A, Tomaru H, Matsumoto R (2011) Molecular and isotopic characteristics of hydrocarbons in sediments and gas hydrate at eastern margin of Japan Sea. In Proceedings of the 7th Conference on Gas Hydrates (ICGH 2011), Edinburgh, Scotland, United Kingdom, 17–21 July 2011.

Hattori S, Nashimoto H, Kimura H, Koba K, Yamada K, Shimizu M, Watanabe H, Yoh M, Yoshida N (2012) Hydrogen and carbon isotope fractionation by thermophilic hydrogenotrophic methanogens from a deep aquifer under coculture with fermenters. Geochem J 46:193–200

Horibe Y, Craig H (1995) D/H fractionation in the system methane-hydrogen-water. Geochim Cosmochim Acta 59:5209–5217

Horita J (2001) Carbon isotope exchange in the system CO_2-CH_4 at elevated temperatures. Geochim Cosmochim Acta 65:1907–1919

Horita J, Wesolowski DJ (1994) Liquid–vapor fractionation of oxygen and hydrogen isotopes of water from the freezing to the critical temperature. Geochim Cosmochim Acta 58:3425–3437

Hsu HW, Postberg F, Sekine Y, Shibuya T, Kempf S, Horanyi M, Juhasz A, Altobelli N, Suzuki K, Masaki Y, Kuwatani T, Tachibana S, Sirono S, Moragas-Klostermeyer G, Srama R (2015) Ongoing hydrothermal activities within Enceladus. Nature 519:207–210

Imachi H, Aoi K, Tasumi E, Saito Y, Yamanaka Y, Saito Y, Yamaguchi T, Tomaru H, Takeuchi R, Morono Y, Inagaki F, Takai K (2011) Cultivation of methanogenic community from subseafloor sediments using a continuous-flow bioreactor. The ISME J 5:1913–1925

Inagaki F, Hinrichs K-U, Kubo Y, Bowles MW, Heuer VB, Hong W-L, Hoshino A, Ijiri A, Imachi M, Ito M, Kaneko M, Lever MA, Lin C-H, Murayama M, Ohkouchi N, Ono S, Park Y-S, Phillips SC, Prieto-Mollar X, Purley M, Riedinger N, Sanada Y, Sauvage J, Snyder G, Susilawati R, Yakano Y, Tasumi E, Terada T, Tomaru H, Trembath-Reichert E, Wang DT, Yamada Y (2015) Exploring deep microbial life in coal-bearing sediment down to ~2.5 km below the ocean floor. Science 349:420–424

Ishibashi J, Noguchi T, Toki T, Miyabe S, Yamagami S, Onishi Y, Yamanaka T, Yokoyama Y, Omori E, Takahashi Y, Hatada K, Nakaguchi Y, Yoshizaki M, Konno U, Shibuya T, Takai K, Inagaki F, Kawagucci S (2014) Diversity of fluid geochemistry affected by processes during fluid upwelling in active hydrothermal fields in the Izena Hole, the middle Okinawa Trough back-arc basin. Geochem J 48:1–13

Kawagucci S, Toki T, Ishibachi J, Takai K, Ito M, Oomori T, Gamo T (2010) Isotopic variation of molecular hydrogen in 20 °C–375 °C hydrothermal fluids as detected by a new analytical method. J Geophysic Res-Biogeosci 115:G03021

Kawagucci S, Ueno Y, Takai K, Toki T, Ito M, Inoue K, Makabe A, Yoshida N, Muramatsu Y, Takahata N, Sano Y, Narita T, Teranishi G, Obata H, Nakagawa S, Nunoura T, Gamo T (2013a) Geochemical origin of hydrothermal fluid methane in sediment-associated fields and its relevance to the geographical distribution of whole hydrothermal circulation. Chem Geol 339:213–225

Kawagucci S, Miyazaki J, Nakajima R, Nozaki T, Takaya Y, Kato Y, Shibuya T, Konno U, Nakaguchi Y, Hatada K, Hirayama H, Fujikura K, Furushima Y, Yamamoto H, Watsuji T, Ishibashi J, Takai K (2013b) Post-drilling changes in fluid discharge pattern, mineral deposition, and fluid chemistry in the Iheya North hydrothermal field, Okinawa Trough. Geochem Geophys Geosyst 14:4774–4790

Kawagucci S, Kobayashi M, Hattori S, Yamada K, Ueno Y, Takai K, Yoshida N (2014) Hydrogen isotope systematics among H_2–H_2O–CH_4 during the growth of the hydrogenotrophic methanogen Methanothermobacter thermautotrophicus strain ΔH. Geochim Cosmochim Acta 142:601–614

Kimura H, Nashimoto H, Shimazu M, Hattori S, Yamada K, Koba K, Yoshida N, Kato K (2010) Microbial methane production in deep aquifer associated with the accretionary prism in Southwest Japan. The ISME J 4:531–541

Knittel K, Boetius A (2009) Anaerobic oxidation of methane: progress with unknown process. Annu Rev Microbiol 63:311–333

Kvenvolden KA (1988) Methane hydrate—a major reservoir of carbon in the shallow geosphere. Chem Geol 71:41–51

Lovley DR (1985) Minimum threshold for hydrogen metabolism in methanogenic bacteria. Appl Environ Microbiol 49:1530–1531

Martini AM, Budai JM, Walter LM, Schoell M (1996) Microbial generation of economic accumulations of methane within a shallow organic-rich shale. Nature 383:155–158

McCollom TM (1999) Methanogenesis as a potential source of chemical energy for primary biomass production by autotrophic organisms in hydrothermal systems on Europa. J Geophys Res 104:30729–30742

McCollom TM (2008) Observation, experimental, and theoretical constraints on carbon cycling in Mid-Ocean Ridge hydrothermal systems. In: Lowell RP, Seewald JS, Metaxas A, Perfit MR (eds) Magma to Microbe: Modeling hydrothermal processes at ocean spreading centers. Geophysical Monograph Series. American Geophysical Union, Washington, D. C., pp 193–213

McCollom TM (2013) Laboratory simulations of abiotic hydrocarbon formation in Earth's deep subsurface. Rev Mineral Geochem 75:467–494

Moran JJ, House CH, Freeman KH, Ferry JG (2005) Trace methane oxidation studied in several Euryarchaeota under diverse conditions. Archaea 1:303–309

Nakai N, Yoshida Y, Ando N (1974) Isotopic studies on oil and natural gas fields in Japan. Chikyukagaku (in Japanese with English abstract) 7(8):87–98

Ono S, Wang DT, Gruen DS, Sharwood-Lollar B, Zahniser MS, McManus BJ, Nelson DD (2014) Measurement of a doubly substituted methane isotopologue, $^{13}CH_3D$, by tunable infrared laser direct absorption spectroscopy. Anal Chem 86(13):6487–6494

Patra PK, Houweling S, Krol M, Bousquet P, Belikov D, Bergmann D, Bian H, Cameron-Smith P, Chipperfield MP, Corbin K, Fortems-Cheiney A, Fraser A, Gloor E, Hess P, Ito A, Kawa SR, Law RM, Loh Z, Maksyutov S, Meng L, Palmer PI, Prinn RG, Rigby M, Saito R, Wilson C (2011) TransCom model simulations of CH_4 and related species: linking transport, surface flux and chemical loss with CH_4 variability in the troposphere and lower stratosphere. Atmos Chem Physic 11:12813–12837

Penning H, Plugge CM, Galand PE, Conrad R (2005) Variation of carbon isotope fractionation in hydrogenotrophic methanogenic microbial cultures and environmental samples at different energy status. Global Change Biol 11: 2103–2113

Proskurowski G, Lilley MD, Kelley DS, Olson EJ (2006) Low temperature volatile production at the Lost City hydrothermal field, evidence from a hydrogen stable isotope geothermometer. Chem Geol 229:331–343

Reeves E, Seewald JS, Sylva SP (2012) Hydrogen isotope exchange between n-alkanes and water under hydrothermal conditions. Geochim Cosmochim Acta 77:582–599

Saito Y, Sakai S, Saito Y, Aoki M, Miyazaki M, Tasumi E, Yamaguchi T, Inagaki F, Takai K, Imach H (2014) Cultivation of anaerobic, syntrophic heterotrophic bacteria with hydrogenotrophic methanogens from deep subseafloor sediments off Shimokita, Japan. In: Proceedings of International Symposium on Microbial Ecology (ISME15). Seoul, Korea, 24–29 August 2014.

Scheller S, Goenrich M, Thauer RK, Jaun B (2013) Methyl-coenzyme M reductase from methanogenic archaea: Isotope effects on the formation and anaerobic oxidation of methane. J Am Chem Soci 135:14975–14984

Schoell M (1980) The hydrogen and carbon isotopic composition of methane from natural gases of various origins. Geochim Cosmochim Acta 44:649–661

Schoell M (1988) Multiple origins of methane in the Earth. Chem Geol 71:1–10

Sekiguchi Y, Kamagata Y, Nakamura K, Ohashi A, Harada H (2000) *Syntrophothermus lopocalidus* gen. nov., sp. Nov., a novel thermophilic, syntrophic, fatty-acid-oxidizing anaerobe which utilizes isobutyrate. Int J Syst Evol Microbiol 50:771–779

Smith DR, Doucette-Stamm LA, Deloughery C, Lee HM, Dubois J, Aldredge T, Bashirzadeh R, Blakely D, Cook R, Gilbert K, Harrison D, Hoang L, Keagle P, Lumm W, Pothier B, Qiu DY, Spadafora R, Vicaire R, Wang Y, Wierzbowski J,

Gibson R, Jiwani N, Caruso A, Bush D, Safer H, Patwell D, Prabhakar S, McDougall S, Shimer G, Goyal A, Pietrokovski S, Church GM, Daniels CJ, Mao JI, Rice P, Nolling J, Reeve JN (1997) Complete genome sequence of *Methanobacterium thermoautotrophicum* ΔH: Functional analysis and comparative genomics. J Bacteriol 179:7135–7155

Stolper DA, Lawson M, Davis CL, Ferreia AA, Santos Neto EV, Ellis GS, Lewan MD, Martini AM, Tang Y, Schoell M, Sessions AL, Eiler JM (2014) Formation temperatures of thermogenic and biogenic methane. Science 344:1500–1503

Stolper DA, Martini AM, Clog M, Douglas PM, Shusta SS, Valentine DL, Sessions AL, Eiler JM (2015) Distinguishing and understanding thermogenic and biogenic sources of methane using multiply substituted isotopologues. Geochim Cosmochim Acta 161:219–247

Sugimoto A, Wada E (1995) Hydrogen isotopic composition of bacterial methane - CO_2/H_2 reduction and acetate fermentation. Geochim Cosmochim Acta 59: 1329–1337

Takai K, Inoue A, Horikoshi K (2002) *Methenothermococcus okinawensis* sp. nov., a thermophilic, methane-producing archaeon isolated from a Western Pacific deep-sea hydrothermal vent system. Int J Syst Evol Microbiol 52:1089–1095

Takai K, Gamo T, Tsunogai U, Nakayama N, Hirayama H, Nealson KH, Horikoshi K (2004) Geochemical and microbiological evidence for a hydrogen-based, hyperthermophilic subsurface lithoautotrophic microbial ecosystem (HyperSLiME) beneath as active deep-sea hydrothermal field. Extremophiles 8:269–282

Takai K, Nakamura K, Toki T, Tsunogai U, Miyazaki M, Miyazaki J, Hirayama H, Nakagawa S, Nunoura T, Horikoshi K (2008) Cell proliferation at 122 °C and isotopically heavy CH_4 production by a hyperthermophilic methanogen under high-pressure cultivation. Proc Natl Acad Sci U S A 105:10949–10954

Tang Y, Perry JK, Henden PD, Schoell M (2000) Mathematical modeling of stable carbon isotope ratios in natural gases. Geochim Cosmochim Acta 64:2673–2687

Thauer RK, Kaster A-K, Seedorf H, Buckel W, Hedderich R (2008) Methanogenic archaea: ecologically relevant differences in energy conservation. Nature Reviews in Microbiology 6:579–591

Umezawa T, Aoki S, Nakazawa T, Morimoto S (2009) A high-precision measurement system for carbon and hydrogen isotopic ratios of atmospheric methane and its application to air samples collected in the Western Pacific region. J Meteorol Soc Japan 87:365–379

Valentine DL, Chidthaisong A, Rice A, Reeburgh WS, Tyler SC (2004) Carbon and hydrogen isotope fractionation by moderately thermophilic methanogens. Geochim Cosmochim Acta 68:1571–1590

Vignais PM (2005) H/D exchange reactions and mechanistic aspects of the hydrogenases. Coord Chem Rev 249:1677–1690

Waldron S, Waston-Craik IA, Hall AJ, Fallick AE (1998) The carbon and hydrogen stable isotope composition of bacteriogenic methane: A laboratory study using a landfill inoculum. Geomicrobiol J 15:157–169

Waldron S, Lansdown JM, Scott EM, Fallick AE, Hall AJ (1999) The global influence of the hydrogen isotope composition of water on that of bacteriogenic methane from shallow freshwater environments. Geochim Cosmochim Acta 63:2237–2245

Walter S, Laukenmann S, Stams AJM, Vollmer MK, Glexner G, Roeckmann T (2012) The stable isotopic signature of biologically produced molecular hydrogen (H_2). Biogeosciences 9:4115–4123

Wang DT, Gruen DS, Sherwood-Lollar B, Hinrichs K-U, Stewart LC, Holden JF, Hristov AN, Pohlman JW, Morrill PL, Konneke M, Delwiche KB, Reeves EP, Sutcliffe CN, Ritter DJ, Seewald JS, McIntosh JC, Hemond HF, Kubo MD, Cardace D, Hoeler TM, Ono S (2015) Nonequilibrium clumped isotope signals in microbial methane. Science 348:428–431. doi:10.1126/science.aaa4326

Whiticar MJ (1999) Carbon and hydrogen isotope systematics of bacterial formation and oxidation of methane. Chem Geol 161:291–314

Whiticar MJ, Faber E, Schoell M (1986) Biogenic methane formation in marine and freshwater environments: CO_2 reduction vs. acetate fermentation—Isotope evidence. Geochim Cosmochim Acta 50:693–709

Yang H, Gandhi H, Shi L, Kreuzer HW, Ostrom NE, Hegg EL (2012) Using gas chromatography/isotope ratio mass spectrometry to determine the fractionation factor for H2 production by hydrogenase. Rapid Commun Mass Spectrom 26:61–68

Yoshioka H, Sakata S, Kamagata Y (2008) Hydrogen isotope fractionation by *Methanothermobacter thermoautotrophicus* in coculture and pure culture conditions. Geochim Cosmochim Acta 72:2687–2694

Submit your manuscript to a SpringerOpen journal and benefit from:

► Convenient online submission
► Rigorous peer review
► Immediate publication on acceptance
► Open access: articles freely available online
► High visibility within the field
► Retaining the copyright to your article

Submit your next manuscript at ► springeropen.com